UNIVERSITÀ
DI PAVIA

Dipartimento di Biologia e Biotecnologie “L. Spallanzani”

Laurea Magistrale in Neurobiologia
Fondazione IRCCS Istituto Neurologico Carlo Besta

Neonatal FC receptor blockade in experimental model of Myasthenia Gravis: ex vivo studies to evaluate secondary effects in splenic lymphoid cells.

Blocco del recettore Fc neonatale nel modello sperimentale di Miastenia Gravis: studi ex vivo per valutare gli effetti secondari sulle cellule linfoidi spleniche.

Relatore:
Prof. Serena Pellegatta, PhD

Correlatore:
Dott.ssa. Elena Rinaldi

Tesi sperimentale di
Fatemehossadat Razavi Khankahdani

Anno Accademico: 2024/2025

UNIVERSITÀ
DI PAVIA

Dipartimento di Biologia e Biotecnologie “L. Spallanzani”

Laurea Magistrale in Neurobiologia
Fondazione IRCCS Istituto Neurologico Carlo Besta

Neonatal FC receptor blockade in experimental model of Myasthenia Gravis: ex vivo studies to evaluate secondary effects in splenic lymphoid cells.

Blocco del recettore Fc neonatale nel modello sperimentale di Miastenia Gravis: studi ex vivo per valutare gli effetti secondari sulle cellule linfoidi spleniche.

Relatore:
Prof. Serena Pellegatta, PhD

Correlatore:
Dott.ssa. Elena Rinaldi

Tesi sperimentale di
Fatemehossadat Razavi Khankahdani

Anno Accademico: 2024/2025

Contents

Content of Figure

Content of Tables

Abstract

Myasthenia gravis (MG) is an autoimmune disease, T-cell dependent and B-cell-mediated, characterized by weakness and fatigability of skeletal muscles due to impaired neuromuscular junction (NMJ) function. In the last years, many drugs have been proposed for the treatment of MG, and it has been authorized the use of Efgartigimod, a human recombinant IgG1 antibody fragment, that binds the neonatal Fc receptor (FcRn) and blocks the IgG recycling. Thus, the level of circulating autoantibodies decreases, leading to clinical benefits in MG patients. Since the FcRn is expressed not only on endothelial cells of vessels, but also on immune cells, the aim of this study was to investigate if Efgartigimod could have any immunological effects, beyond its established role in IgG reduction. The research particularly focused on splenic lymphoid cells in an experimental model of MG (EAMG), by integrating cellular and molecular approaches.

EAMG was induced in mice by multiple subcutaneous injections of purified *Torpedo californica* AChR (TAChR) and Efgartigimod or PBS was administered biweekly intraperitoneally after the second boost. Clinical evaluations were performed to assess the severity of symptoms until the end of the experiment. *Ex vivo* analysis was conducted to quantify circulating anti-AChR antibodies in serum and muscle AChR content in Efgartigimod-treated mice and PBS-EAMG mice. Flow cytometry was conducted to assess any variations in the percentage of naïve, effector memory, and central memory for the T cells lineage (CD4 and CD8). Germinal center B cells, plasma cells, and long-lived plasma cells were selected for the B cell lineage. Additionally, selected miRNAs (miR-150, miR-146a, and miR-486) were isolated, and expression levels were compared among the EAMG group, Efgartigimod-treated mice, and healthy controls. Moreover, the expression of the mRNA target was analyzed.

Results demonstrated the efficacy of Efgartigimod in dampening the clinical symptoms of EAMG, and a lower concentration of anti-AChR antibodies was detected in the serum of Efgartigimod-treated mice. In parallel, a higher content of muscle AChR was found in treated mice. This data demonstrated the effectiveness of an anti-FcRn in ameliorating EAMG. Flow cytometry analysis on splenocytes revealed an increase in $CD8^+$ T cells and a decrease in $CD19^+B220^+$ B cells. Interestingly, data revealed a higher percentage of plasma cells ($CD138^+$ $TACI^+$) and long-lived plasma cells ($CD138^+TACI^+$ $CD19^-B220^-$) in Efgartigimod-treated mice compared to PBS-EAMG. Because this increase was not associated with an increase in anti-AChR antibodies, it could be argued that these plasma cells may have a non-pathogenic phenotype with immunoregulatory properties. Expression profiling of miRNA revealed that

even if all of them were increased in EAMG mice, only miR-150 was significantly higher. Efgartigimod treatment seemed to restore the expression of miR486 significantly to the HD level. No differences were observed in mRNA expression levels of IRAK and TRAF6 (targets of miR-146a), SMAD2 and PTEN (target of miR-486), and FOXP1 and MYB (targets of miR-150).

These findings demonstrate that Efgartigimod not only decreases pathogenic IgG levels but also acts on other immune mechanisms. To better outline the secondary effects of the anti-FcRn administration, additional studies should be conducted to clarify the mechanisms of action of Efgartigimod on B cells differentiation in PC and extend the analysis to more miRNA involved in the immune response.

Keywords: Myasthenia Gravis (MG), Autoimmune disorder, Flowcytometry, MicroRNA.

Abbreviation

Abbreviations	***Meaning***
MG	Myasthenia gravis
EAMG	Experimental Autoimmune Myasthenia Gravis
EFGA	Efgartigimod-treated Experimental Group
HD	Healthy group
EOMG	Early-onset Myasthenia gravis
LOMG	Late-onset Myasthenia Gravis
AChR	acetylcholine receptor
nAChR	Nicotinic acetylcholine receptors
TAChR	Torpedo AChR (purified from Torpedo californica)
NMJ	neuromuscular junction
Tfh	helper T cells
Tregs	regulatory T cells
MuSK	muscle-specific tyrosine-kinase
LRP4	low density lipoprotein receptor-related protein
CFA	Complete Freund adjuvant
IFA	Freund's incomplete adjuvant
Ct	Cycle threshold
IRAK1	interleukin-1 receptor-associated kinase 1
TRAF6	Tumor Necrosis Factor Receptor-Associated Factor 6
FOXP1	Forkhead Box Protein P1
MYB	Myeloblastosis Oncogene
SMAD	Mothers Against Decapentaplegic Homolog
PTEN	Phosphatase and Tensin Homolog
TGFB	Transforming Growth Factor Beta

1 Introduction

1-1 Myasthenia gravis(MG)

Myasthenia gravis (MG) is a chronic autoimmune disease where the immune system attacks communication between nerves and muscles, such as acetylcholine receptors (AChR). This pathological mechanism results in loss of these receptors and damages muscle membranes, thereby affecting the responses of muscles (Mantegazza Renato et al., 2018). In most of the MG cases, about 80-85% of the antibodies are against acetylcholine receptors, while around 5-8 percent developed antibodies against muscle-specific kinase (MuSK). A few groups, less than 1%, show antibodies for another protein, called Lrp4. About 10% of MG patients do not have antibodies against any other known targets (Grob D. et al., 2008).

Clinically, signs in MG translate into muscle weakness and fatigability, especially in ocular muscles, often associated with diplopia and ptosis(Alshekhlee A et al., 2009) MG also affects bulbar muscles, leading to dysphagia, dysarthria, and respiratory problems, and weak limb muscles.

1.1.1 Epidemiology

Many epidemiological features of MG have been identified through extensive studies, which indicate some specific features. First, a very prominent feature is the bimodal age distribution, showing two peaks of incidence: early-onset MG (EOMG) characterized by patients in their thirties (30-39), with a higher incidence among females, and late-onset MG (LOMG), more common in older adults, especially males. Furthermore, the existence of ethnic differences in the prevalence of MG among racial groups is an interesting epidemiological feature (Gilhus NE et al., 2015).

Changes in the incidence of MG over time and across geographical regions have prompted discussions as to whether the differences represent an actual difference in etiology or were the result of methodological bias. Epidemiologic investigations of rare and heterogeneous conditions like MG face many challenges, such as small sample sizes, divergent inclusion criteria, and heterogeneous data sources, which affect comparability. While national registries covering national yields serve as an excellent basis for an epidemiological investigation, these registries are often lacking in many countries (Uzawa A et al., 2021).

The introduction of novel therapeutic interventions such as acetylcholinesterase inhibitors, immunosuppressive drugs, intravenous immunoglobulin, and improved respiratory care has lowered the mortality associated with MG since the early 1900s. However, with these gains,

the mortality still lies in a band of 5%-9%, with a slight male predominance (Gilhus NE et al., 2015). The data analysis of the Network and Information Security (NIS) repository for 2000-2005 showed an all-hospital mortality of 2.2%, while this number increased to 4.7% for those who were in MG crisis. Important variables for mortality are age and respiratory failure(Alshekhlee A et al., 2009).

1.1.2 Risk factors: genetic architecture, geo-epidemiology, and the environment

MG pathogenesis involves a complex interplay of genetic and environmental influences. Several genes regulate immune modulation in Tregs and Tfh, activated by cytokines like IL-17 and IL-21, or signaling mechanisms such as BAFF, tumor necrosis factor (TNF), and interferon-gamma (IFNG)(Gilhus NE et al., 2015).Increased MG susceptibility is linked to HLA genes, PTPN22, CTLA4, and others, with specific HLA associations for AChR-MG (HLA B8-DR3) and MuSk-MG (DQ5-DR14)(Phillips LH, 2004; Zhong H et al., 2019). Family patterns suggest MG patients have a higher autoimmune disease, highlighting genetic susceptibility (Avidan N et al., 2014). Concordance rates are observed at 35% in Monozygotic twins and 5% in Dizygotic twins, while environmental factors remain unclear (Punga T et al., 2016).

The thymus gland likely plays a key role in MG, Epstein-Barr virus-infected B cells have been implicated. Other viral infections, including West Nile virus and Zika virus are associated with MG (Gilhus NE et al., 2015). Cancer immunotherapy, particularly immune checkpoint inhibitors can trigger MG and related autoimmune conditions (Benfaremo et al., 2018; Kao et al., 2018). Thymic disorders such as dysfunction, hyperplasia, or thymomas may significantly impair immune tolerance, contributing to specific Mg like thymoma-associated MG (TAMG) and acetylcholine receptor antibody-positive MG ($AChR^+$ MG) (Marx.A et al., 2010; Payne AS et al., 2005).

1.1.3 Age and Gender

MG appearance ages are known to differ between genders: Early-onset MG (EOMG) appears to affect women predominantly, whereas late-onset MG (LOMG) pervades men more. The description of the disorder can fluctuate in men and women of all age groups: "a disease of young women and old men." The youngest case reported to have undergone onset was at 1 year(Seybold M & Lindstrom J., 1981) , the oldest at 98 years (J.C. Keesey, 2002). Women usually display peak onset ages of 20 to 39 years (Beghi E et al., 1991), whereas men display them at 50 to 70 years (J.C. Keesey, 2002).

The age distribution of females shows a consistent bimodal pattern displaying both early-onset and late-onset peaks, males tend to show a solitary late-onset peak.

Gender is one of the main epidemiological risk factors determining the emergence of autoimmune diseases, since the immune system is sexually dimorphic(Santos et al., 2016). Most autoimmune disorders have a sex-based difference; for example, MG is more prevalent in women than men. In such case of early-onset MG, the female-to-male ratio is 3:1(Phillips LH, 2004). Different effects of pregnancy on disease have been observed: 41% with exacerbation of disease, 29% with remission of symptoms, and 30% with no change (Avidan N et al., 2014)

The immune responses are influenced by hormones at both innate and adaptive levels, as well as across the cellular pathway. Estrogen suppresses autoimmune-regulator gene in the thymus, due to increasing autoreactive T cell release, consequently, MG occurs more frequently in young women than in men. Estrogen exerts its effects via various mechanisms, including classical receptor-mediated and non-classical mechanisms pathway. These mechanisms involve both genomic(nuclear) and non-genomic (extranuclear) interactions with receptors, regulating gene expression, protein modifications, and cellular. A potential therapeutic approach using specific estrogen-receptor blockers may yield a better outcome in certain autoimmune diseases compared to generalized treatments(Cunningham M & Gilkeson G., 2011) .

1.1.4 Clinical feature and classification of MG

The clinical classification issued from the MG Foundation of America (MGFA), includes a discussion of specific muscles, such as oculomotors, oropharyngeal, limb muscles, and further detection based on severity (Jaretzki A et al., 2000).

Class I consist of Weakness of the ocular muscles while Class II indicated mild weaknesses beyond ocular muscles. Within this category II-a Involves limb and axial muscles, whereas II-b includes possible oropharyngeal muscles and respiratory involvement. Class III denotes Moderate weakness with III-a Primarily affecting distal limb and axial muscles and III-b involving oropharyngeal and respiratory muscles. Class IV signifies Severe muscle weakness with IV- effects on limb and axial muscles and IV-b on oropharyngeal and respiratory muscles. Class V is characterized by the need for intubation or mechanical ventilation, excluding routine postoperative care, while patients requiring a feeding tube without intubation are classified under IV-b (WHO, 2015).

Patients with MG are indeed usually classified into separate subgroups according to numerous criteria:

(1) Age of Onset: This includes juvenile-onset (≤18 years), early-onset (19–50 years, often seen in young women), and late-onset (>50 years).
(2) Thymoma Present: This specifies MG associated with thymoma.
(3) Associated Antibodies: This differentiation depends upon the presence of antibodies against AChR, or less frequently, against Musk. Recent targets include LRP4 (Zisimopoulou P et al., 2014) and Agrin, an extracellular matrix protein (Gasperi C et al., 2014).
(4) Clinical Phenotype: This divides into ocular MG or generalized forms of MG.

Autoantibody	Onset age	Thymus
AChR	< 50 years	Hyperplasia common
AChR	>50 years	Atrophy common
AChR	Any	Thymoma
MuSK	Any	Normal
LRP4	Any	Normal
Non detected	Any	Variable
Variable	Any	Variable

Table 1- Classification of MG Subtypes by Onset Age and Antibody Specificity. *MG is classified into several subtypes according to the time at which symptoms appear and the antibody present. Early-onset MG is defined as symptoms before 50 years of age, while late-onset MG is defined as symptoms developing after 50 years of age. Thymoma-associated MG occurs in people with tumors of the thymus gland, which possibly can cause dysfunction of the immune system. MuSK-MG is characterized by the presence of muscle-specific kinase antibodies that block the channel of communication between nerves and muscles. Finally, LRP4 MG pertains to antibodies directed against the low-density lipoprotein receptor-related protein 4, which is a critical part of the neuromuscular transmission (Zisimopoulou P et al., 2013).*

1.1.5 Pathology and mechanism

1.1.5.1 Neuromuscular Junction (NMJ)

The NMJ is the point of contact between the terminal end of a spinal motor neuron and a muscle fiber. The whole sequence begins with an action potential stimulating the opening of voltage-gated $Ca2^{+}$ channels, leading to the influx of calcium ions ($Ca2^{+}$) into the nerve terminal (Koneczny I et al., 2013). The influx of $Ca2^{+}$ leads to the exocytotic release of ACh from synaptic vesicles into the synaptic cleft. ACh diffuses rapidly across the cleft and binds to AChRs on the postsynaptic membrane, opening cation-permeable channels, thus causing a localized depolarization. Depolarization leads to the activation of neighboring voltage-gated sodium channels (VGSC), which in turn gives rise to potential action in the muscle fiber Acetylcholinesterase (AChE) as it hydrolyzes ACh in the synaptic cleft from excessive activation, regulates contraction of muscles. Additionally, NMJ efficiency improves through specialized folds in the postsynaptic membrane, which increase AChRs and VGSCs. This enhances signal transmission and muscle activation (Figure 1a)(Robert L. Ruff & Robert P. Lisak, 2018).

Several proteins, including the heparan sulfate proteoglycan Agrin, ARE SECRETED from nerves, regulate NMJ assembly and activity, as well as three muscle-cell-specific proteins: Dok7, LRP4, and rapsyn (Hubbard & Gnanasambandan, 2013). Agrin binds to LRP4, activates MuSK, which plays a crucial role in promoting AChR clustering via Rapsyn and DOK-7. This interaction, promoting the accumulation of AChRs and postsynaptic specialization ensuring efficient neuromuscular transmission (Figure1) (LAZARIDIS K ET AL., 2020).

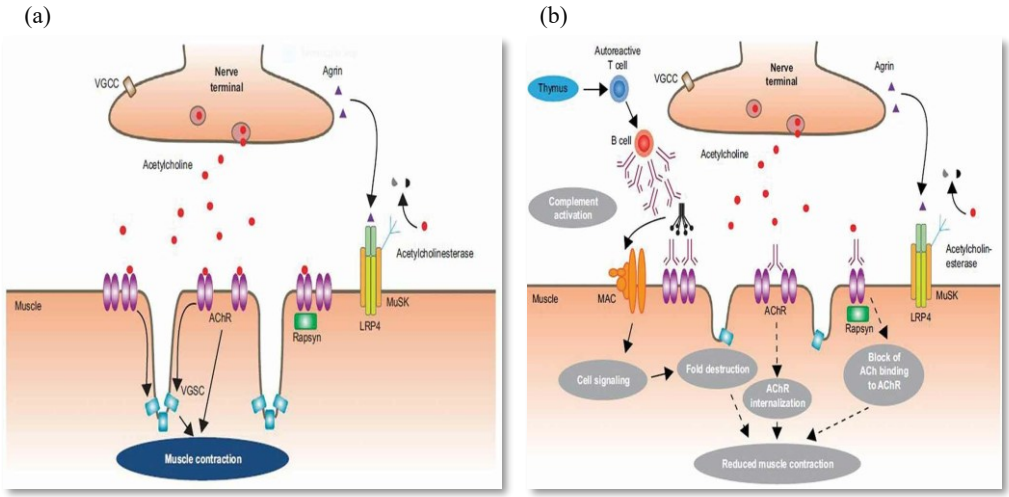

Figure 1- Neuromuscular Junction*: Healthy State vs. Pathology in MG. (a) Healthy NMJ. The action potential that is triggered at the presynaptic nerve terminal results in the openin of voltage-dependent Ca2+ channels,*

1.1.5.2 Acetylcholine receptor (AChR) and pathology in MG

The two principal varieties of AChRs may be classified as nicotinic receptors and muscarinic receptors; with nicotinic receptors being defined first, as the receptors that operate as ion channels and allow the flow of sodium and calcium ions, while muscarinic receptors are G-protein-coupled receptors involved with modulation of various types with either inhibitory or excitatory effects as a result. The nicotinic AChR in muscle is a heteropentamer formed of two alpha (α) subunits, one beta (β) subunit, and one delta (δ) subunit. In the fetal isoform, the δ-subunit is substituted by an epsilon (ε) subunit in the adult isoform (Figure 2a). Each of the AChR subunits exhibits a prominent extracellular N-terminal domain which features a characteristic one of thirteen residues bordered by cysteine residues (C130-C144 in human γ-subunit and C128-C142 in human ε-subunit) (Hakan Cetin et al., 2020).

Additionally, the structure comprises four transmembrane domains (M1-M4) and a cytoplasmic loop domain that varies in length and amino acid composition, localized between the M3 and M4 transmembrane helices (145 amino acids in the human γ-subunit and 128 amino acids in the human ε-subunit; see Figure 2b). Differences in the functional properties of fetal and adult

AChRs have been attributed to the structural discrepancies between the γ-subunit and the ε-subunit (Hakan Cetin et al., 2020). Anti-AChR antibodies can be found in nearly 80% of MG patients and are categorized as polyclonal. Antibodies interact with the extracellular domains of the AChR and affect the disease pathology in a variety of ways (see Figure 2b). Anti-AChR antibodies are primarily composed of IgG1 and IgG3 Isotypes, which can trigger the complement cascade. The artificial complement reaction causes receptor endocytosis, impairment of postsynaptic functioning, injury to the membrane, and antigenic modulation. Therefore, it more significantly reduces receptor availability and interrupts signal transduction (Kaori Noridomi et al., 2017; Robert L. Ruff & Robert P. Lisak, 2018; Romi F et al., 2005)

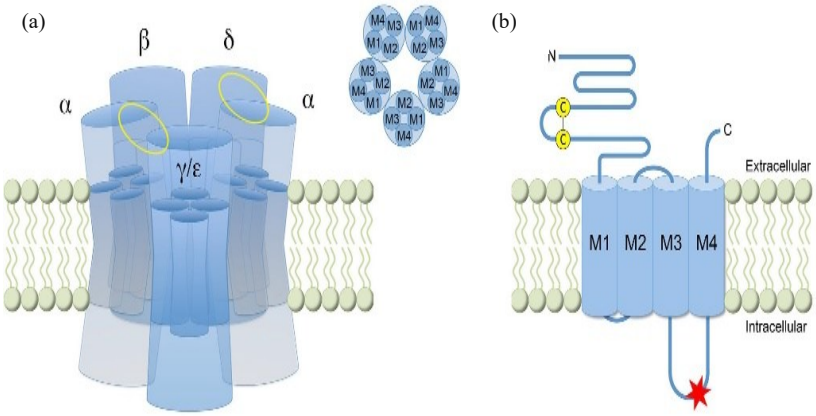

Figure 2- AChR structure. *The AChR is a pentametric ligand-gated ion channel composed five subunits, each ones containing four transmembrane domains(M1-M4) AChR mediated neurotransmission at NMJ. In MG, autoantibody targeting leads to receptor degradation, impaired neuromuscular transmission and muscle fatigue (Jacob, 2018).*

Another major mechanism of pathogenesis involves antigenic modulation, which promotes the speedier internalization and destruction of AChRs through the crosslinking of these receptors by bivalent antibodies (Zisimopoulou P et al., 2013, Kaori Noridomi et al., 2017). This crosslinking reduces the AChR present at the postsynaptic membrane, a loss that is not fully compensated by the concomitant increased synthesis of AChR due to the heightened degradation mediated by the autoantibodies. On rare occasions, some of the anti-AChR antibodies can directly block the binding site for acetylcholine and thus inhibit AChR signals (Zisimopoulou P et al., 2013) Of note, in MG, the anti-AChR antibodies against the α-subunit of the AChR are more pathogenic than those against the other subunits, and the pattern of the specific epitope of these antibodies may influence disease severity.(Kaori Noridomi et al., 2017).

1.1.5.3 Muscle specific tyrosine kinase MG (MuSK MG)

The MuSK gene, which runs from chromosome 9q31.3, comprises 11 constitutive exons and 5 alternative exons. these give rise to six transcript variants through alternative splicing. MuSK

is expressed in skeletal muscle, However, MuSK expression has also been reported in several tissues, including small intestine, testis, bladder, lung, and to a very small scale in the brain, specifically within the epithalamus. MuSK is a typical transmembrane type I glycoprotein characterized by extracellular immunoglobulin-like domains and a frizzled-like cysteine-rich domain that promotes interactions with LRP4 thereby facilitating homodimerization. These components are linked to a cytoplasmic tyrosine kinase domain. Agrin boosts the contacts between MuSKs and LRP4 whereas the binding of Dok7 strengthens dimerization of MuSK, which is crucial in activating the kinase domain as well as NMJ formation (D.M. Valenzuela et al., 1995; Kaminski et al., 2024; Maartje G.M. Huijbers et al., 2014).

In MG, MuSK autoantibodies are found in about 5-8% of cases and are primarily of IgG4 subclass, considered immuno-incompetent because they do not activate complement nor bind to Fcγ receptors. The antibodies are functionally monovalent and specific for the N-terminal Ig-like1 domain of MuSK, interfering with its interaction with LRP4 and Agrin. As a result, AChR clustering and neuromuscular transmission are impaired, producing MG symptoms. Interestingly, monovalent MuSK antibodies inhibit that activation induced by Agrin while probably bivalent antibodies activate the MuSK kinase partially. The overall pathogenic effect depends on these antibody activities' interaction (Dana L.E. Vergoossen et al., 2021; Higuchi O et al., 2011; Hoch W. et al., 2001).

1.1.5.4 LRP4 MG

Between 1-50% of individuals without AChR or MuSK autoantibodies are reported to have autoantibodies against LRP4 (Higuchi O et al., 2011; Pevzner et al., 2012; S. Zhang et al., 2008). LRP4 belongs to the LDL receptor family and has a large extracellular N-terminal region with multiple repeats of epidermal growth factor and low-density lipoprotein receptor-like domains, a transmembrane domain, and a short C-terminal region that lack any recognizable catalytic motif (Huybrechts et al., 2022).

LRP4 plays a key role in the activation and phosphorylation of MuSK, and the signaling of these factors induces AChRs aggregates and NMJ formation. The process prevents proper clustering of AChRs at the NMJ, thereby compromising synaptic transmission and leading to muscle weakness. Moreover, LRP4 autoantibodies also contribute to NMJ fragmentation and a reduction in synaptic vesicles further worsening MG symptoms (Chen et al., 2016).

1.1.5.5 Agrin MG

Agrin is an extracellular matrix protein that facilitates motor neuron-induced accumulation of AChR at the NMJ. Agrin autoantibodies have been found in some MG patients (Gasperi et al.,

2014; Michael H. Rivner et al., 2020) often together with antibodies against either AChR or MuSK (Yan F et al., 2018). Agrin interacts with a few muscle membrane proteins, including LRP4, dystroglycan, and laminin, and thereby plays a major role in NMJ formation, maintenance, and regeneration (Witzemann V et al., 1992) .

1.1.5.6 Thymoma-associated MG (TAMG)

Thymoma is often associated with paraneoplastic neurological syndromes. TAMG is named a subtype of anti-AChR-MG. The thymus is a primary organ that serves as a major differential and educational institution for T-lymphocytes. There is a cortex and medulla within the organ; the first affording positive selection and negative selection of thymocytes is accomplished (McGuire LJ et al., 1988).

Thymic epithelial cells (TELC) are the parts of the structures of the medulla that present tumor-specific antigens (TSAs) such as a few subunits of the AChRs that are vital for establishment of central tolerance and avoidance of developing autoimmunity. Myoid cells in the thymus also incorporate AChRs. Thymuses commonly reveal distortion and act as the effector organs in AChR positive MG patients. Thymoma patients usually have a poorer prognosis (P. Strobel et al., 2008). The Worldwide health organizations (WHO) categorize thymomas into various types; these include six of them A, B, C AB, B1, B2, and B3. Among this classification, those thymomas with a more significant lymphocyte component will have a stronger association with MG, especially AB, B1, and B2 types.

Type	Histological description
A	Medullary thymoma
AB	Mixed thymoma
B1	Predominantly cortical thymoma
B2	Cortical thymoma
B3	Well-differentiated thymic carcinoma
C	Thymic carcinoma

Table 2- ***Histopathological Classification of Thymoma Cells Based on Morphology and T Lymphocyte Levels (WHO Guidelines, 2015).*** *The histopathological classification established by the World Health Organization (WHO) is predicated on the morphology of epithelial cells and the quantity of associated T lymphocytes, which serve as a marker for the biological activity of thymoma cells (WHO, 2015).*

1.1.6 Diagnosis

Overwork-induced muscle weakness specifies MG. Patients may present asymmetric ptosis and diplopia with orbicularis oculi being the most frequently afflicted muscle. Asymmetric ptosis can be examined by two tests: lid fatigability test and curtain test, both based on Hering's law which states that the apparent movements of one eye result from the super imposition of conjugate movement (where both eyes move together) and disjunctive movements (where the

two eyes move in opposite directions). The diplopia accompanying MG is due to weakness of various extra-ocular muscles and changing with time provides the distinction from other disorders (Carr AS et al., 2010).

Serological assays serve as the holy grail of diagnosis of MG, being found to be highly sensitive and specific for the generalized form of the disease, albeit losing some sensitivity in ocular MG. Neurophysiological tests such as repetitive nerve stimulation (RNS) and single-fiber electromyography (SF-EMG) are the key diagnostic modalities, with SF-EMG possessing the highest sensitivity, but requiring expert interpretation (Hans Frykman & Pankaj Kumar, 2021). Needle EMG is beneficial for differential diagnosis of MG that detects problems with motor nerves, muscles, or communication between the two (Pasnoor et al., 2018), while the ice pack test is a rapid, non-invasive test to assess ptosis with diagnostic value comparable to that of SF-EMG (T.Rossen & Rousseff, 2021).

1.1.7 Treatment

Two major approaches are employed for MG treatment: symptomatic and immunosuppressive therapy. A symptomatic treatment is meant to improve neuromuscular transmission and may include acetylcholinesterase inhibitors, for example pyridostigmine, which acts to increase the availability of Ach at the NMJ(Zhao C et al., 2021).

Immunosuppressive treatments deal with the underlying pathological immune response present in MG and include corticosteroids, azathioprine, and more recent additions like rituximab and eculizumab(Carmelo Rodolico et al., 2020). Additionally, thymectomy has also been shown to have a steroid-sparing effect and improve clinical outcomes in patients with non-tymomatous MG, as demonstrated by the international randomized controlled trial of thymectomy in MG (MGTX) (Hobson-Webb LD et al., 2017).

Approach	**Therapeutics**	**Mechanism of Action**	**Most Substantial Adverse Effects**
Modulation of Neuromuscular Transmission	Pyridostigmine Amifampridine	Cholinesterase inhibition Enhanced acetylcholine release	GI hypermotility Paresthesias, rare
General Immunomodulation	Plasma exchange IVIg	Antibody removal Multiple pathways	Catheter-related infection Headache, rare thrombosis
General Immunomodulation	Corticosteroids Azathioprine Tacrolimus, Cyclosporine Mycophenolate Methotrexate	Multiple pathways B and T cell inhibition Block T cell activation and replication Selective T cell blockade Increased T cell apoptosis	Multiple adverse effects Hepatotoxicity Nephrotoxicity Teratogenicity Hepatotoxicity
Complement Inhibition	Eculizumab Ravulizumab	Inhibits C5 cleavage, inhibit C5 cleavage, block C5b6 formation	Increased risk of encapsulated bacterial infection Like eculizumab
FcRn Inhibition	Zilucoplan Efgartigimod Rozanolixizumab	Reduce circulating antibody cRn inhibition FcRn inhibition	Headache, nausea, diarrhea Not specific Not specific

B Cell Ablation	Rituximab	Binds CD20	Infusion reactions, long-term lymphocyte depletion

Table 3- Therapies for Myasthenia Gravis: Mechanism of action and adverse effects. *MG management includes therapeutic modalities that focus on their mechanism of action, related drugs, and most significant adverse effects. These therapies include, but are not limited to neuromuscular transmission agonists, general immunomodulators, and complement inhibitors. There are also FcRn inhibitors and B-cell ablation. Each modality has unique drugs with specific functions-from antibody removal to selective T cell blockade-and potential side effects like hepatotoxicity, nephrotoxicity, and increased bacteremia risk. This thorough classification will serve as a good reference in both the therapeutic efficacy and safety considerations in MG management. (J-clin invest)*
Abbreviations*: ChE: Cholinesterase ; GI: Gastrointestinal ;IVIg: Intravenous immunoglobulin*

A complementary therapeutic strategy negates complement activation, one of the downstream pathogenic pathways directly activated by AChR antibodies. The neonatal Fc receptor (FcRn), a molecule resembling class I MHCs, is vital for the recycling of immunoglobulin G (IgG), thereby extending its half-life to nearly four times that of other non-recycled immunoglobulin classes such as IgM or IgA (Hamaguchi y et al., 2015). Within the cell, the Fc portion of an IgG binds to two FcRn receptors in the endosomal acidic milieu. This interaction preserves IgGs from lysosomal degradation and allows their release back into the extracellular environment when physiological pH conditions return (Chen d et al., 2017) . Therefore, FcRn sustains IgG autoantibodies' availability in IgG-mediated disorders, including generalized MG. The management of FcRn is a rational therapeutic point of view regarding the proposed mainpathogenic mechanism of generalized MG (Mantegazza r et al., 2022).

Efgartigimod is a well-tolerated treatment option with a safety profile, with infection as a side effect. It is an Fc fragment of human IgG1, has nanomolar affinity to FcRn, receptor mainly expressed on endothelial cells, to outcompete endogenous IgG binding at both physiological and acidic pH. This mechanism leads to sustained reduction in circulating IgG, and, as consequence, decrease in pathogenic autoantibodies in the context of autoimmune diseases (Yun Yang et al., 2024). Drug regulatory agencies approved the use of Efgartigimod in MG to downregulate levels of circulating anti-AChR antibody (Newland AC et al., 2019; Renato Mantegazza & Fiammetta Vanoli, 2022). Indeed, the ADAPT study (A Phase 3 Study to Evaluate the Efficacy and Safety of Efgartigimod in Adults with Generalized MG), validated that Efgartigimod resulted in consistently increased muscle strength and alleviation of symptoms in patients with generalized MG, thereby underscoring its promise for treating autoimmune neuromuscular disorders (Howard et al., 2021).

1.2 Overview of the immune System

1.2.1 Immune response

Disruption of an immune system (IS) is a very elaborate complex assembly of lymphoid organs, various cell types, humoral factors and cytokines. Its pivotal function making the host immune

is clearly observed when abnormal conditions arise in this system leading to overwhelming infection and tumors in cases of immunodeficiencies as well as hypersensitivity activities manifested in allergic and autoimmune conditions. The immune defense is classified into two principal types based on the response rate and specificity: innate and adaptive immunity, and, importantly, thoroughgoing interactions occur between the two (Janeway et al., 2001).

Innate immunity consists of physical barriers, chemical and microbiological barriers, as well as neutrophils, monocytes, macrophages, complement proteins, cytokines, and proteins of the acute phase, all bringing about immediate protection. Indeed, the fact that the innate immune response is extraordinarily conserved, even in the most primitive organisms, shows that it has a central role in survival (Metchnikoff, 1887). In fact, adaptive immunity is different from innate immunity in that it usually occurs in more evolved organisms and involves antigen-specific responses by effector T lymphocytes and T and B lymphocytes.

The innate immune response is very fast, but it is not very selective, which may lead to damage to normal tissues; the adaptive response, however, is very well-honed but often takes several days and sometimes even weeks to manifest fully. Adaptive immunity includes an important feature: it creates memory, so that reinforcements are faster and stronger changes during a second encounter with the same antigen (Delves & Roitt, 2000a). The sequence of stages in this two-step process starts with presenting an antigen to T or B cells, activating and differentiating them in lymphoid tissues. The effector phase follows, where activated T cells migrate to the site of infection and antibodies released by activated B cells into the blood stream and tissues are used to embargo the invading pathogen. All these combined components make up an overall defense mechanism that works together to protect the host from a wide range of pathogens while maintaining a delicate balance to avoid self-harm (Delves & Roitt, 2000b).

1.2.2 Role of thymus in immune system

The thymus is an important organ for T cell maturation, facilitating a controlled process takes place where some hematopoietic stem cells from the bone marrow develop into thymocytes. This process occurs in thymic cortex and medulla, under the control of thymic epithelial cells (TECs), which are necessary for T cell selection (Mélanie A Cron et al., 2017).

Thymocytes start as double-negative (DN) cells with no CD4 or CD8 co-receptors. Following the four stages (DN1, DN2, DN3, and DN4) distinguished by various surface markers, thymocytes eventually express functional TCRs with positive signals for maturation. The rearrangement of TCR beta chain in so-called DN3 stage thymocytes leads to precursor TCR

complex formation and initiates beta selection and further development into double-positive (DP) CD4/CD8 thymocytes. The DP cells are subjected to positive selection in the cortex of the thymus through interaction with self-antigens presented by cortical MHC-committed epithelial cells; those that show preferential reactivity will migrate to the medulla where negative selection is taking place, driving ones that show strong self-reactivity to death by apoptosis to prevent autoimmunity. Thymocytes then differentiate into single-positive (SP) cells expressing CD4 or CD8 at exit from the thymus to mature into T cells in the peripheral immune system (Referred Figure 3) (Balandina et al., 2005; Treuting, 2018).

Thymic output is age-dependent; its activities would matter most during the fetal and early childhood, then it would gradually decline during early adulthood. Therefore, the infants with poor thymic development might have some possibilities to be not so good in terms of immune function. (Fujii Y et al., 1986).

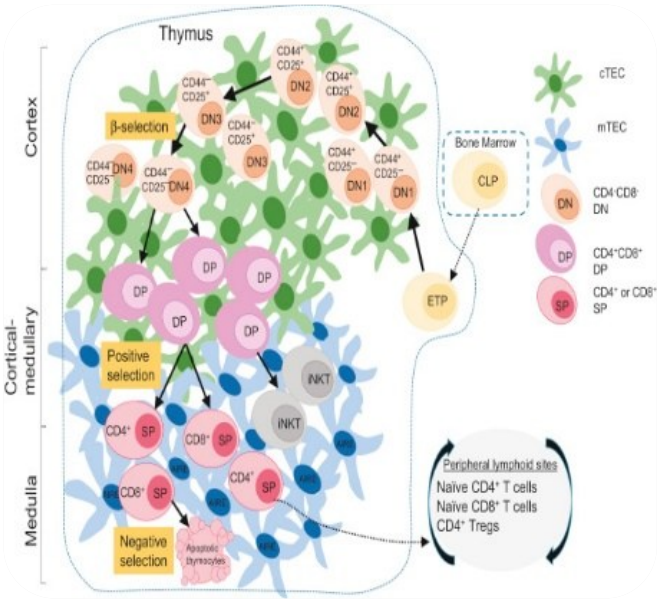

Figure 3- *T-cell development in the thymus-* *T-cell development in the thymus. Common lymphoid progenitor (CLP) cells from the bone marrow migrate as early thymic precursors (ETP) and through four steps (DN1-L4) differentiate into double-negative (DN) thymocytes (TAN-ORANGE) characterized by expression of CD44 and CD25. At the DN3 stage, the expression of TCRβ allows maturation into double-positive (DP) thymocytes (PINK) characterized by CD4 and CD8 expression. Positive selection produces single-positive (SP) CD4 or CD8 T cells (MAROON). In the medulla, SP T cells undergo negative selection to remove autoreactive cells. Surviving SP T cells enter peripheral blood and lymphoid tissues as naive CD4+ and CD8+ T cells, including CD4 T regulatory cells (Comparative anatomy and histology) (Balandina et al., 2005).*

1.2.3 Thymus pathologies in MG

Thymic functional and morphological changes in MG patients, together with improvement post-thymectomy, underscore its importance in the pathogenesis of the disease. The hyperplastic thymus in MG (an increase in the size and number of thymic cells) (Refer to Figure

4), is characterized by a complex immune response involving B lymphocytes producing anti-AChR antibodies, autoreactive T lymphocytes, antigen-presenting cells (APC), and the AChR itself (Leprince C et al., 1990; Wang Z-Y et al., 1993). Critical features of thymic hyperplasia include the appearance of germinal centers (GC), which B-lymphocyte proliferation and selection. GCs could thus be employed to quantify hyperplasia in the thymic sections: two or fewer GCs mean a state of low hyperplasia while three or more GCs mean conspicuous hyperplasia (Rozen Le Panse et al., 2006)

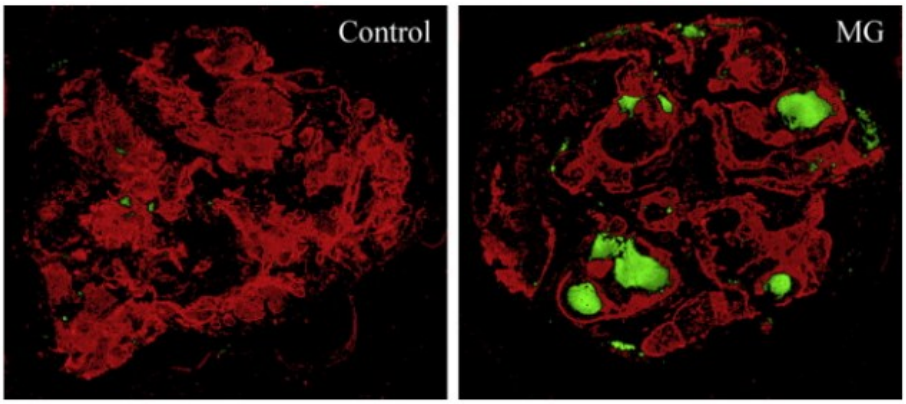

Figure 4- Germinal centers in MG patients compared to non-MG patients. *Germinal centers (GCs) formation in the hyperplastic thymus of MG patients. Immunohistochemically analysis of thymic sections from a non- MG patient (left) and an MG patient (right). The epithelial network was stained in red with anti-keratin antibody and GCs in green with anti-CD21 antibody (Mélanie A Cron et al., 2017).*

1.2.3 The role of spleen in immune response

The spleen, the largest of secondary lymphoid organs in the human body (Figure 5a), is involved in various immunological functions, in addition to hematopoiesis and clearance of red blood cells. Its architecture makes it possible to filter blood effectively, removing pathogens as well as abnormal cells, and allowing between antigen-presenting cells and lymphocytes. (Morris O. Dailey, 2002) . The innate and adaptive immune systems come together within the spleen through the red pulp and white pulp. In rodents, this is separated between marginal zone and in humans, the perifollicular zone. White pulp is where most of the immune work is done, while the functions of the red pulp are quite different. Unlike lymph nodes, immune cells and antigens reach the spleen via the bloodstream. It is in the upper left abdomen near the stomach. Rodent spleens are elongated, weighing 100-200 mg for 2-4-month-old mice (Treuting, 2018) . While blood circulates freely through the marginal zone, the white pulp is isolated from direct circulation, requiring specific signals for entry of its cells. Thus, the marginal zone is interfaced with innate and adaptive responses: macrophages capture pathogens, and marginal-zone B cells may become activated into antigen-presenting cells and IgM-secreting plasma cells (Figure 5c).(Boldin et al., 2011) .

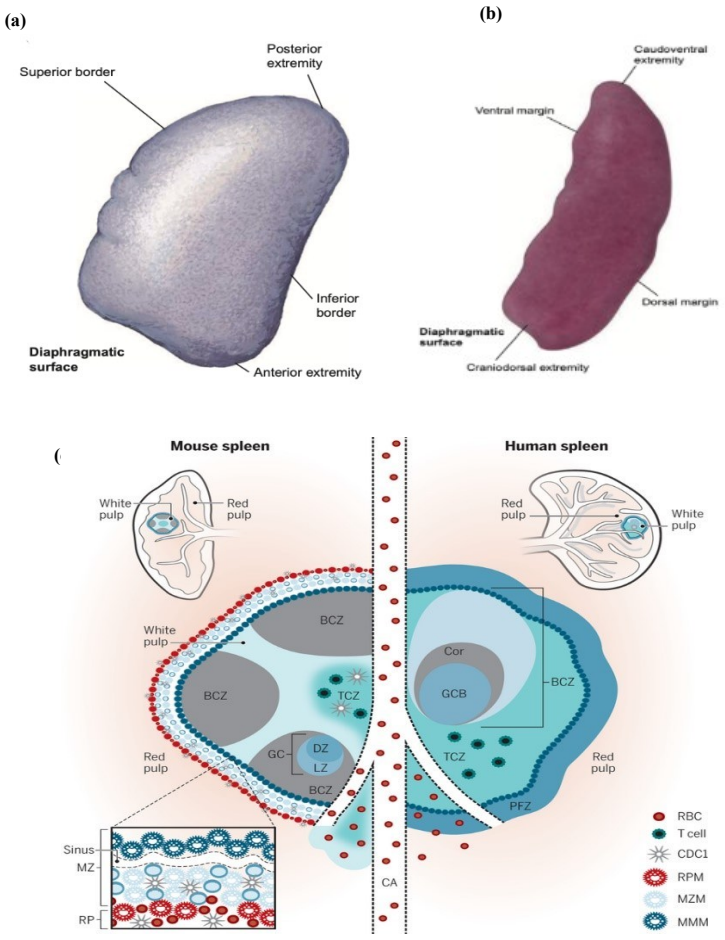

Figure 5- Schematic representations of the splenic immune architecture in mouse and human Spleen. *(a) Diagram of the human spleen. (b) Diagram of the mouse spleen. Adapted from "Comparative Anatomy and Histology: A Mouse, Rat, and Human Atlas." (c) Immune architecture of the spleen in mice (left) and humans (right) at steady state shows notable differences in T cell zones (TCZ) and B cell zone (BCZ) arrangements. In mice, macrophage subsets form a ring around the white pulp (WP), while in humans, MZB cells encircle activated B cells in germinal centers (GC). The relationship between the mouse marginal zone and the human peri-follicular zone (PFZ) is unclear due to limited imaging studies. (Morris O. Dailey, 2002)*

1.2.4 Role of lymph nodes in immune response

Lymph consists of a fluid that escapes from interstitial spaces of tissues and is gradually collected by lymphatic vessels until flowing back into circulation through the thoracic duct (Figure 6). In response to foreign microorganisms, antigen-presenting cells, such as dendritic cells, actively seek the antigens at the site of infection, process them, and migrate to the lymph nodes to activate T and B lymphocytes. The lymphatic vessels are essentially the "information superhighway" conveying important messages about the local inflammatory status. (von Andrian UH & Mempel TR, 2003). Like other autoimmune diseases, lymphoid tissues assume an important role in the autoimmune mechanisms pertaining to the pathology in MG. Indeed, the lymph nodes act as key microenvironments in which immune cells, mainly T and B

lymphocytes, undergo activation and clonal expansion in response to autoantigens, including those that target AChR at the non-junctional membrane. This immune activation ultimately results in producing autoantibodies contributing significantly to the muscle weakness and fatigue seen in MG. Certainly, inflammatory cytokines and mediators released by activated lymphocytes within the lymph nodes may further promote the autoimmune response and trigger pathways involved in the pathophysiological processes of MG (Miriam L. Fichtner et al., 2020).

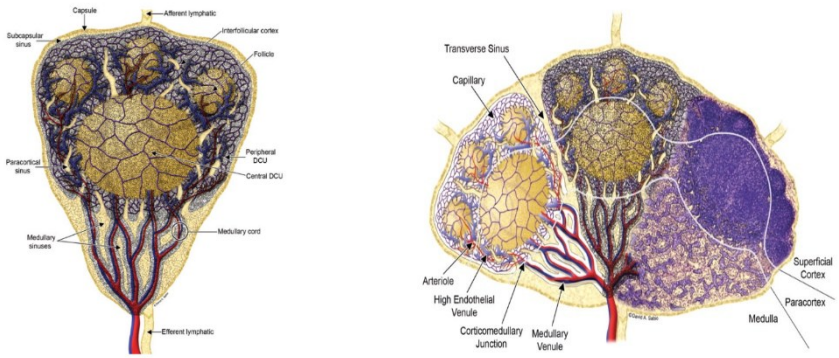

Figure 6- The Lymph node's architecture. *A midsagittal section reveals three lymphoid lobules, each associated with an afferent lymphatic vessel. The lymph node is compartmentalized into superficial cortex (follicles and interfollicular cortex), paracortex (deep cortex), and medulla (medullary cords and sinuses). The left lobule contains arterioles and venules within the medullary cords. Arterioles branch within the paracortical cords and interfollicular cortex, forming capillary beds. Capillaries are present in follicles and the central DCU, but their density is reduced in these regions. (Comparative anatomy and histology: A mous, Rat and Humn atlas, (Piper M. Treuting et al., 2017.).*

1.3 microRNAs

1.3.1 Regulation of miRNA biogenesis and turnover in the immune system

miRNAs are short RNA sequences, generally 19 to 25 nucleotides long, that play an important role in the regulation of gene expression at the post-transcriptional level. They target various mRNAs and are involved in several biological processes, including differentiation, cell proliferation, and immune responses (Chen et al., 2020). MiRNAs function downstream of various signaling pathways to influence transcription factors and the chromatin structure. They represent a class of small non-coding RNA molecules that are essential for several critical biological functions, including innate immunity, inflammatory responses, hematopoiesis, and metastasis. Mis-regulation of the expression of miRNAs by either upregulation or downregulation tends to interfere with cellular homeostasis and integrity (Mark P. Boldin et al., 2011).

Circulating microRNAs (miRNAs) are released into the extracellular environment and can be detected in many biofluids, such as blood serum and plasma. Recently, these circulating miRNAs have been accepted as easily obtainable biomarkers found in different body fluids that

are distinct in their profiles and concentrations in relation to different human diseases, including the conditions of autoimmunity. MicroRNAs play an important role in the immune response by influencing the maturation of immune systems, the proliferation of relevant immune cells-as well as their differentiation resulting in specific subtypes-and the regulation of apoptosis in every crucial checkpoint of immunological significance. Any perturbation in these activities may lead to autoimmune disease via mechanisms mostly involving aberrant regulation of miRNA expression and its downstream effects (Renato Mantegazza et al., 2019).

1.3.2 miRNA-146a function, involvement innate immunity and inflammatory response

miRNA-146a is located on chromosome 5 in the MIR3142HG host gene, playing an important role in physiological processes of the innate immune response, where Toll-like Receptors (TLRs) identify microbial components and subsequently provoke immune reactions. These 11 distinct types of TLRs (from TLR-1 to TLR-11) expressed across different cell types can interact with a wide variety of ligands. For instance, the activation of post-receptor signaling pathways in innate immune responsiveness evoked by TLRs occurs via either the MyD88 signaling or the TRIF pathway. miRNA-146a, however, targets significant signaling proteins downstream in the MyD88-dependent pathway; hence being crucial in innate immunity (Akira et al., 2006). Additionally, miR 146a plays a crucial role in autoimmune disorders such as MG, where it's dysregulation is associated with immune system imbalance.

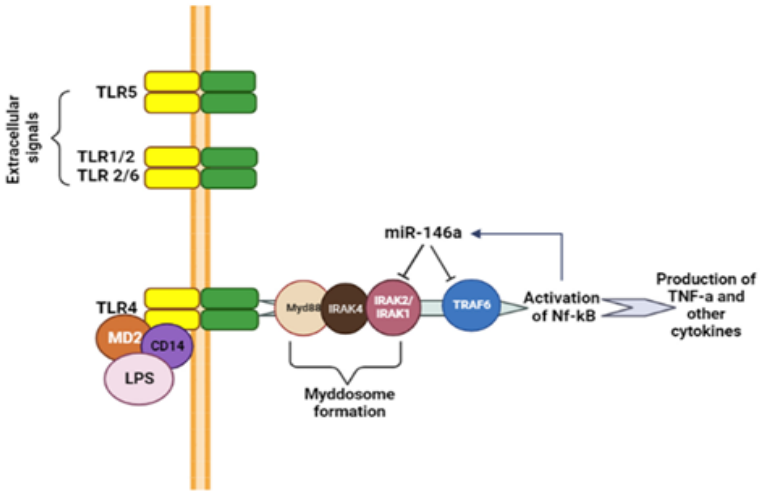

Figure 7-miRNA 146-a regulates targets *in the MYD88-dependent signaling pathway. The pathway that gets activated leading up to NF-xB and MPK activation has been activated by most toll-like receptors (TLRs) except TLR3, which activates the TRIF pathway. Functional TLR signals play a significant role in the eradication of pathogens, and they help induce the production of the type 1 interferon (IFNs) and antiviral proteins. While the MyD88 pathway is the leading path, both TLR pathways may cause damage to the host and thus require careful regulation. miRNA 146-a play an important role in maintaining the balance of this innate response. (Esaba et al., 2014)*

miRNA-146a is to inhibit adapter proteins interleukin-1 receptor-associated kinase 1 (IRAK1)-related to the IL-1 receptor 1-and TRAF6-to TNF receptor 6, all of which are major modulating proteins in signaling pathways of TLR and IL-1 receptors. In MG, reducing miRNA 146a expression led to increased IRAK1 and TRAF6 activity, caused to inflammation and immune dysregulation. With the inhibition of pro-inflammatory mediators' secretion and blockade of TLR signals, miRNA-146a upregulates protein expression in knockout cell lines. TRAF6 is essential for the differentiation of myeloid cells, and its overexpression relates to acute myeloid leukemia expansion, indicating that miRNA-146a might be a tumor suppressor gene. (Figure 7) (Chen et al., 2016).

1.3.3 miR-150 expression in B cells of the mantle one of Germinal centers

miR-150 is an immune microRNA regulating immune processes like proliferation, apoptosis, and differentiation of NK, T, and B cells (Xiao C et al., 2007) Its dysregulation acts as a diagnostic marker for autoimmune disorders and is reported to influence the initiation and progression of disease. Located on chromosome 19q13.33, miR-150 is produced predominantly, in lymphoid tissues like lymph nodes, spleen, and thymus (Punga T et al., 2014). It shows a high level in mature B and T lymphocytes but is expressed at a very low level in progenitor cells (Monticelli S, Ansel KM, Xiao C, et al., 2005). Thus, these results indicate that maximal expression is seen during lymphocyte development (Zhou B et al., 2007b).

miR-150 is critical for B-cell regulation, controlling their proliferation, differentiation, development, and antibody production by targeting genes such as MYB, FOXP1, survivin and FLT3 (Figure 8) (Bousquet M et al., 2013,Ying W et al., 2016, Xue-Ping L, et al., 2023). B cells, the physiological effectors of the host's immune system, develop from common lymphoid progenitor (CLP) cells through several distinct developmental stages. B progenitor cells (pro-B) transition to precursor (pre-B) cells, to immature B cells expressing membrane-bound IgM. Upon exiting from the bone marrow at the transitional 1 (T1) stage-while still functionally immature cells advance to transitional 2 (T2), mature (M), and marginal zone (MZ) B cells en route to the spleen (Hardy, 2004). Follicular B cells, MZ B cells, and B1 cells are the main subsets of mature B cells, whereas follicular and MZ B cells are jointly referred to as B2 cells (Zhou B et al., 2007a).

miR-150 is mainly upregulated during T-cell maturation; however, its effects on mature CD8 or CD4 T-cell differentiation are relatively weak (Zhou B et al., 2007a). In addition to this, miR-150 is subsequently down-regulated upon differentiation of naive T cells to effector Th1 and Th2 cells (Monticelli S, Ansel KM, & Xiao C, 2005). Specifically, miR-150-5p is a

methylated marker in MG, as it is expressed at greater levels in MG-thymuses, which are associated with thymic B cells (Punga AR et al., 2018). Its aberrant expression by immune cells has been correlated with quite a few autoimmune diseases, including multiple sclerosis (MS) (Z.B. Hu et al., 2018); myasthenia gravis (MG) (Mélanie A Cron et al., 2017), systemic lupus erythematosus (SLE) (Zhou H et al., 2013), rheumatoid arthritis (RA) (Hu Z et al., 2017), and primary Sjögren's syndrome (pSS) (Chen et al., 2020).

Evidently, miR-150 is vital for immune regulation, as it targets c-MYB, FOXP1, FLT3, survivin, and components of the B-cell receptor signaling cascade, which are all critical in B-cell development and immune function (Lutwyche JK et al., 2001).The c-myb proto-oncogene codes for a transcription factor that is critically required for proliferation, differentiation, and survival of hematopoietic cells (Oh IH & Reddy EP, 1999).

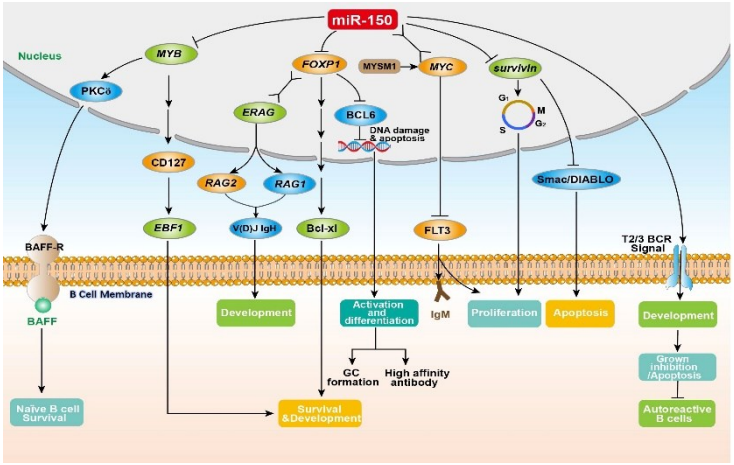

Figure 8- The physiological miR-150 regulation. *miR-150 regulatied the B cells populations, which affecting their proliferation, differentiation, development, and antibody production by inhibiting several target genes such as MYB, FOXP1, survivin, and FLT3. These genes are relevant to the G2/M phase of the B cell cycle and enhance T2/T3 B cell receptor signaling* (Balandina et al., 2005).

In the case of MG, thymic hyperplasia with infiltration of ectopic B cells is a prominent aspect, which occurs alongside dysfunctional Tregs with normal numbers. MiR-150 is significantly upregulated in MG, affecting both B cells and T cells by promoting immune dysregulation. In B cells, mir-150 is associated with activation in ectopic germinal centers, while in T cells, it impacts on survival and differentiation, disrupting immune tolerance. In contrast, thymectomy reduce miR-150 level, correlating with symptom improvement in patients (Balandina et al., 2005).

1.3.4 miRNA-486-5p: A regulator of immune function and inflammation

miR-486-5p is a microRNA most prominently visible in muscle tissues, where it exists in both cytoplasm and nucleus; it is extremely rich in human plasma, especially in small extracellular vesicles. This microRNA plays a crucial role in regulating key signaling pathways essential for the cellular processes of proliferation, migration, angiogenesis, and apoptosis (Adrianna Douvris et al., 2022). This microRNA found in muscle tissue (Small EM et al., 2010), circulating in plasma at elevated concentrations (Bayés-Genis A et al., 2018). It is also concentrated in small extracellular vesicles and has been associated with signaling pathways relevant to various cancers (ElKhouly AM et al., 2020), in addition to non-cancerous conditions like skeletal muscle disorders.

miR-486-5p is transcribed from an intron within the ANK1 locus on chromosome 8p11.21. The Ankyrin 1 gene is found here, which is expressed in erythroid tissues, with high expression shown in myoblasts during myogenesis and in skeletal muscle (Alexander MS et al., 2011) . It is also significantly present in cardiac muscle, with moderately lower amounts in lung tissue. The phosphatase and tensin homolog (PTEN) function as a tumor suppressor protein, and its expression is meticulously controlled at the various levels (Brito MB et al., 2015). PTEN has been recognized as the first validated target of miR-486-5p (Small EM et al., 2010). PTEN, as a lipid phosphatase, negatively regulates the phosphatidyl-inositol-3-kinase (PI3K)/Protein kinase B (Akt) signaling pathway by dephosphorylating the intracellular messenger and PI3K product phosphatidyl-inositol-triphosphate (PIP3) back to PIP2. Thus, this inhibits various cellular processes, including proliferation, migration, survival, and angiogenesis (Figure 9) (Gomez-Manzano C et al., 2003).

Additionally, in autoimmune diseases such as MG, miR-486-5p directly targets Smad1/2/4, and inhibit TGF-β signaling, thereby reducing immune regulation, which allow pro-inflammatory responses to persist (Xiaohua Yan et al., 2009). Smad proteins play a crucial role in transmitting TGF-β signals, regulating immune homeostasis, and suppressing excessive inflammation. Their upregulation in MG may act as a compensatory mechanism against excessive immune activation and chronic inflammation (Xiaohua Yan et al., 2009).

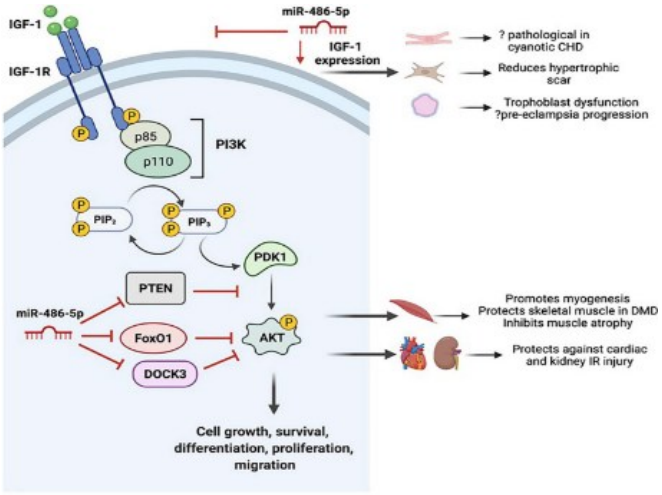

Figure 9- miR-150 in B cell regulation. *The miR-150 is crucial in regulating B cells, affecting their proliferation, differentiation, development, and antibody production by inhibiting several target genes such as MYB, FOXP1, survivin, and FLT3. These genes are relevant to the G2/M phase of the B cell cycle and enhance T2/T3 B cell receptor signaling. Critical proteins involved are MYB, PKCδ, BAFF, BAFF-R, CD127, EBF1, FOXP1, RAG1, RAG2, Bcl-xl, BCL6, MYSM1, MYC, FLT3, IgM, and Smac/DIABLO (Yue-Zi Hu, Qiao Li, Xue-Ping L, et al., 2023).*

2 Aim of research

In the last years, many new biological drugs have been suggested for treatment of MG. Specifically, an anti-FcRn drug (Efgartigimod) has been approved for AChR+ MG patient treatment, thanks to its ability to block the recycling of IgG and, consequently, also of autoantibodies. However, since FcRn is expressed also on immune cells and mediates other biological effects, further studies may help to understand if this drug could act on other molecular mechanisms. Therefore, this research aimed to investigate the indirect effects of blockage of neonatal Fc receptor (FcRn) in the experimental mouse model of autoimmune Myasthenia Gravis (EAMG), with a focus on splenic lymphoid cells.

The first step was evaluating the efficacy of Efgartigimod in ameliorating the clinical symptoms of EAMG and the effects on circulating anti-AChR antibody concentration in serum and muscle AChR content. Then, the project investigated the secondary effects of Efgartigimod on immune cells of the spleen, a fundamental lymphoid organ involved in the autoimmune response.

Flow cytometry was employed to analyze splenic immune cell populations. Variations in percentage of naïve, effector memory and central memory were investigated for the T cells lineage (CD4 and CD8), whereas germinal center B cells, plasma cells and long-lived plasma cells were selected for the B cell lineage.

Additionally, selected miRNAs (miR-150, miR-146a, and miR-486) were isolated, and expression levels were compared among EAMG group, Efgartigimod-treated mice and healthy controls. Moreover, the expression of mRNA target was analyzed.

3 Material and methods

3.1 TAChR extraction from electric organ of Torpedo California

Torpedo California has a phenomenal quantity of acetylcholine receptor proteins in its NMJ and especially in the electric organ, the modified neuromuscular structure (Hess GP, 1979). For extraction of the electric organ of *Torpedo California*, Buffer A, Buffer B, and Wash Buffer must all be prepared (Table 4).

Buffer	Component
Buffer A	Sodium phosphate (pH: 7.4, 10 mM)
	0.5 mM EDTA
	0.1 M NaCl
	0.02% NaN_3
Buffer B	4 % Triton
	1 mM PMSF

Table 4- Preparation of Buffers for Acetylcholine Receptor (AchR) Extraction from Torpedo californica. *The buffers contain sodium phosphate for stabilizing the pH, EDTA for chelating divalent metal ions, NaCl to ensure ionic balance, NaN_3 to inhibit microbial growth, PMSF serving as a protease inhibitor, and sodium cholate to solubilize membrane proteins, thereby enhancing the effective extraction of AchR.*

The electric organs of *Torpedo California* were thawed slowly according to the alkali-stripped membrane protocol with minor modifications. All subsequent steps were performed on ice. The organs were weighed and cut, homogenized using an Omni Mixer for 3 minutes at speed 4 with a volume of Buffer A equivalent to the initial organ weight. If the homogenate was not well-formed, an additional one-minute at speed 5 was performed. Then 30 seconds using a Ystral homogenizer were performed.

The homogenate was transferred to ultracentrifuge tubes, and centrifuged at 32000 rpm for 1 hour at 4°C. The pellet was re-suspended in half of the initial weight of ice-cold distilled water ($V=\frac{1}{2}$ Wg) and adjusted to pH 11 using 1N NaOH. After another centrifugation at 32000 rpm for 30 minutes at 4°C. The pellet was resuspended in $\frac{1}{8}$ volume ($V=\frac{1}{8}$ Wg) of Buffer B and homogenized again.

The solution was incubated overnight at 4°C on the shaker and ultracentrifuged at 32000 rpm for 1 hour at 4°C. The supernatant was collected and placed in a dialysis chamber and dialyzed against Buffer A - Triton 1% for 3 hours at 4°C with shaking. The buffer was gradually changed to Buffer A - Triton 0.5% for 2 hours and followed by Buffer A - Triton 0.05% overnight.

The next day, the supernatant was extracted via syringe, rinsed to recover the full volume, transferred to a 15 mL falcon tube, and stored at -80°C.

3.2 Induction and evaluation of EAMG's mice

EAMG was induced in 6 to 8 weeks- old C57BL/6J mice from Charles Rivers Laboratories (Calco, Italy). The mice were kept in a temperature-controlled room (20-22 °C) on a 12-h light/dark cycle with free access to food and water.

- ***Animal immunization***

Subcutaneous immunization was performed using 20 µg of purified TAChR, diluted in PBS and mixed with CFA (1:1 ratio Difco). The total administered emulsion volume was 200 µl/mouse. After the first immunization, two TAChR booster doses were administered on post-immunization day 30, and day 60, each consisting of 20 µg of TAChR emulsified in incomplete Freund's adjuvants (200 µl/mouse) for the EAMG induction (Canan Ulusoy, 2017). Each animal was weighed and scored at the beginning of each experiment, twice a week until the end of the experiment, or twice daily, if severe weakness was observed, by blind investigators, unaware of the treatments. The study was terminated 13 weeks after initial immunization.

- ***EAMG clinical evaluation***

From the first immunization onward, animals were monitored to evaluate disease onset and clinical severity. Animals were scored twice a week by assessing their ability to grasp the top grid of a cage while being gently dragged by the tail. Scores were based on posture, muscular weakness at rest and after exercise, general fatigue and tremor. Post-exercise weakness in mice lasted less than 30 seconds. Scores were assigned as follow: grade 0, normal strength and no muscle weakness, even after exercise; grade 1, normal at rest but fatigability or weakness (tremor or inability to raise head or hunched posture) observed after exercise; grade 2, clinical signs of weakness present at rest; grade 3, severe clinical signs of weakness: i.e., no ability to grip, hindlimb paralysis, respiratory distress/apnoea; grade 4, humane endpoint/sacrifice due to very severe clinical signs of weakness.

Disease presence was confirmed via intraperitoneal injection of Prostigmine at 0.75 mg, temporarily improving clinical symptoms. Before immunizations and treatment, lower concentrations of anesthesia (2% isoflurane in a 60:40 N_2O:O_2 mixture, at a flow rate of 0.8 l/min) were used. Euthanasia was performed via carbon dioxide inhalation, after which blood was collected for circulation anti-AChR antibody quantification. The spleen was harvested and processed for flow cytometry analysis. Carcasses were stored at -80ºC for subsequent receptor levels determination.

- ***Treatment administration***

Efgartigimod (0.20 mg/kg) and sterile PBS were administered biweekly to assess its therapeutic efficacy in EAMG mouse model, by intraperitoneal administration.

3.3 Ex vivo analysis

- ***Organ harvest: spleen***

The spleen was collected in sterile PBS and processed as follows. The protocol began with filtering through the cell strainer and crushing the spleen with a syringe cap to form a single-cell suspension which was washed with sterile PBS. The suspension was collected in a 50 mL sterile falcon tube, and additional PBS was used to maximize cell recovery. Centrifugation was performed at 300 RCF at 4°C for 5 minutes, after which the supernatant was discarded, and the pellet was resuspended in 3 mL of ACK lysis buffer to lyse red blood cells. The suspension was transferred to ice for 5 minutes. Sterile PBS was added to dilute ACK, followed by another centrifugation 300 RCF at 4°C for 5 minutes. The pellet was then re-suspended in 5 mL of RPMI 1640. Cell counting was performed using a Bürker chamber with a 1:10 dilution in Trypan Blue (10 µl cell; 90 µl Trypan Blue) to assess viability. The pellets were centrifuged again, and the cells were frozen in 1.5 mL cryovials containing 900 µL of FBS for nutrients and 100 µL of DMSO to prevent ice crystal formation. Samples were stored at -80ºC for further analysis.

- ***Serum anti-AchR antibody measurement***

To detect of anti-mouse AChR antibodies the radioimmunoprecipitation assay was used. Terminal serum samples were collected and incubated overnight with muscle AChR extracted from naïve mice and labeled with [125I] α-bungarotoxin (BTX). Antibody-AChR complexes were precipitated using secondary rabbit polyclonal anti-mouse IgG in excess and incubated at RT for 2.5 hours. After centrifugation (3,000 rpm for 10 min at 4°C), the pellet was washed twice with phosphate buffer containing Triton X-100, and [125I] α-BTX-labeled complexes were counted by gamma-counter. Values obtained from control samples (unlabeled α-BTX in excess) were subtracted from the test samples to provide accurate calculations of antibody titer in picomoles of [125I] α-BTX-binding sites per milliliter of serum.

- ***Determination of muscle AChR content***

To analyze the amount of AChR in muscle tissues mice, the radioimmunoprecipitation assay was used. Initially, the carcasses were weighed and homogenized for one minute at high-speed using four volumes of homogenization buffer containing 0.1 M NaCl, 10 mM NaN_3, 0.01 M

EDTA, 0.01 M EGTA, 0.01 M iodoacetamide, 1 mM PMSF, 1 mM sodium phosphate buffer, pH 7.5. The extract was centrifuged at 15,000 rpm for 30 minutes at 4°C, and the pellet was further homogenized in one volume of the same previous buffer. Triton X-100 was added at 10% concentration to solubilize AChR from membranes. Subsequently, extracts were incubated for 4 hours at 4°C with agitation. Finally, centrifuged again (15000 rpm ,30 minutes at 4°C). The supernatant was collected and centrifuged at 26000 rpm for 30 minutes at 4°C, to discard any fat on the interface. Muscle AChR levels were quantified by immunoprecipitation assay. Two parallel 0.1 mL aliquots of the muscle AChR extract were incubated with 0.2 pM [125I] α-BTX, then added the high titer serum of EAMG-mice to each sample and incubated overnight at 4°C to allow for antibody binding. Complexes were precipitated with the addition of excess rabbit anti-mouse IgG (Sigma) and were centrifuged for 10 minutes at 3000 rpm at 4°C. The pellets were washed twice with phosphate buffer containing Triton X-100 to elute unbound material. The bound [125I] α-BTX was counted on a gamma-counter (PerkinElmer). Results were reported as femtomoles of toxin-binding sites/gram of carcasses. Non-specific binding was subtracted using control extracts pre-incubated with unlabeled α-BTX.

3.4 Flow cytometry analysis of splenocytes

For flow cytometry staining, frozen aliquots of cells were thawed in 37°C water bath and assessed for viability by Trypan Blue. Approximately 1-2×10^6 viable splenocytes in PBS were incubated with live-dead dye (FVD - eFluor 506, 1:1000 in PBS). Then, mice Fc receptor block (unlabeled CD16/CD32 monoclonal antibody, 0.5 µg/tube) was applied.

The following antibodies were used for the characterization of B- and T-cell subpopulations: B cells ($CD19^+B220^+$) [CD19–PE-Cyanine7; B220–PE], Plasma cells (PC) ($CD138^+TACI^+$) [CD138–Brilliant Violet 421; TACI/CD267–APC], Long-lived plasma cells (PCLL) ($CD19^-B220^-CD138^+TACI^+$) [$CD19^-$–PE-Cyanine7; $B220^-$–PE; CD138–Brilliant Violet 421; TACI/CD267–APC], Effector memory CD4 T cells (CD4EM) ($CD4^+CD44^+CD62L^-$) [CD4–PerCP-Cyanine5.5; CD44–NovaFluor Blue 610-70S; $CD62L^-$–PE], Effector memory CD8 T cells (CD8EM) ($CD8^+CD44^+CD62L^-$) [CD8–Pacific Orange; CD44–NovaFluor Blue 610-70S; $CD62L^-$–PE],Naïve CD4 T cells (CD4 naïve) ($CD4^+CD44^-CD62L^+$) [CD4–PerCP-Cyanine5.5; $CD44^-$–NovaFluor Blue 610-70S; $CD62L^+$–PE],Naïve CD8 T cells (CD8 naïve) ($CD8^+CD44^-CD62L^+$) [CD8–Pacific Orange; $CD44^-$–NovaFluor Blue 610-70S; $CD62L^+$–PE],Central memory CD4 T cells (CD4CM) ($CD4^+CD44^+CD62L^+$) [CD4–PerCP-Cyanine5.5; CD44–NovaFluor Blue 610-70S; $CD62L^+$–

PE],Central memory CD8 T cells (CD8CM) ($CD8^+CD44^+CD62L^+$) [CD8–Pacific Orange; CD44–NovaFluor Blue 610-70S; $CD62L^+$–PE](Figure 10).

Flow cytometry analysis (NxT Flow Cytometer- Thermo Fisher) was performed on viable cells determined using FCS-A/SSC-A and FVD detection. Single gating was performed via SSC-H/SSC-A. Antibody concentrations were optimized through prior titration and the FMO method was used to gate positive and negative populations.

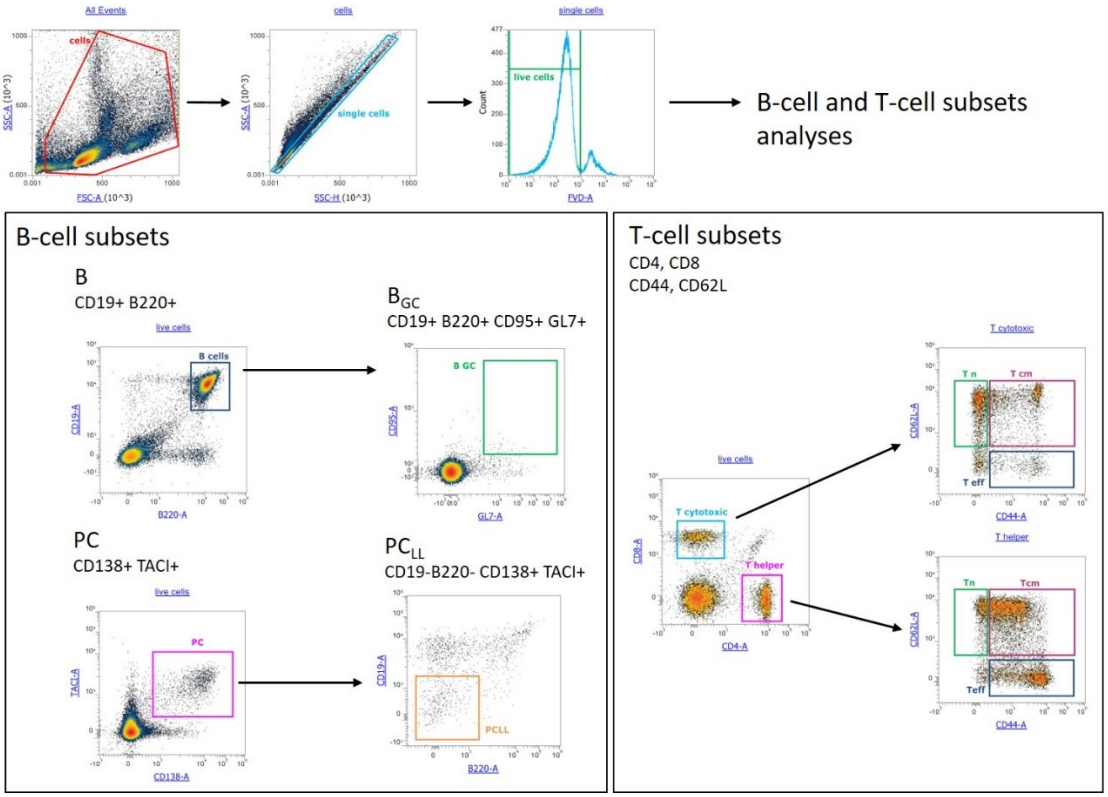

Figure 10- Flow Cytometric Workflow for Immunophenotyping of B and T Cell Populations. *The sequential gating strategy identified B cell population and T cell subsets.*

3.5 miRNA isolation and purification

Investigations into molecular biology emphasized non-coding RNA, focusing on three miRNAs: miR-146a, miR-150, and miR-486. These miRNAs were selected to assess their role in myasthenic pathology by measuring their expression levels in spleen of experimental animals. Expression levels of the target miRNAs were normalized using U6 (J. Zhang et al., 2013), a small nuclear RNA with stable expression across various biological situations, providing reliable internal control.

- ***mirVANA kit isolation***

The first step of the mirVana miRNA Isolation Kit protocol (Table 5) was sample lysis in a denaturing lysis buffer. Acid-Phenol: Chloroform extraction was performed, to provide early purification while removing most of the DNA. (Official Website: Thermo Fisher Scientific, n.d.). To ensure a high yield of intact RNA, the tissue was obtained to minimize the time between procedural steps.

Component	Storage
miRNA wash solution (1)	Room temperature
Wash solution (2/3)	Room temperature
lysis/binding buffer	4° C
miRNA homogenate additive	4° C
Acid-phenol: Chloroform	4° C
Elution solution	Any temperature
Filter cartridge	Room temperature
collection tube	Room temperature

Table 5- Reagents Provided with Kit and Storage. *The kit contains: miRNA wash solution 1, Wash solution 2/3, lysis/binding buffer, miRNA homogenate additive, Acid-phenol: Chloroform and Elution solution, filter cartridge, collection tube (Official Website: Thermo Fisher Scientific, n.d.)*

Wash solutions are prepared as follows: (a) miRNA Wash Solution 1: 21 mL ACS grade 100% ethanol was added to the labeled container and mixed well. (b) miRNA Wash Solution 2/3: 40 mL ACS grade 100% ethanol was added to the labeled container and mixed well.

The first step involved preparing and counting spleen cells, which were resuspended in DMEM and centrifuged at 300 RCF, for 5 minutes at 4°C to precipitate and separate the cells from the supernatant. After centrifugation, the supernatant was carefully removed.

Depending on the cell count, 300-600 µL Lysis/Binding Solution was added to pellet. miRNA additive (1/10th volume of lysate volume) was incorporated, mixed thoroughly, and set on ice for 10 minutes. Acid-Phenol: Chloroform, in volume equal to the lysate, was then added, mixed by vortexing for 30-60 seconds, and Centrifuge at 10,000 ×g for 5 to achieve phase separation. To recover the aqueous phase, 1/3 volume of 100% ethanol was added and mixed vigorously. The lysate/ethanol mixture was then applied to Filter Cartridge inside a collection Tube in volumes up to 700 µL per application. Centrifuge was performed for 15 seconds at 10,000 ×g to pass the mixture through the filter. To filter the flow-through, two-thirds of the total volume with 100% ethanol was added at room temperature and mixed thoroughly. Each sample required one Filter Cartridge placed into available Collection Tubes. The filtrate/ethanol mixture was pipetted onto the second Filter Cartridge up to 700 µL applied per filtration step. Centrifugation was performed at 10,000 ×g (about at 10,000 rpm). For 15 seconds to allow passage through the filter. The flow-through was discarded, and the process was repeated until all the filtrate/ethanol mixture had passed through the filter. Next, 700 µL Wash Solution 1 was added

to the Filter Cartridge and centrifuge for 5-10 seconds or vacuum pressure was applied to facilitate passage through the filter. The flow-through was discarded, and the Filter Cartridge remained in the same Collection Tube.

Then, 500 µL Wash Solution 2/3 was added and passed through the Filter Cartridge as in the previous step. And again, a second 500 µL aliquot of Wash Solution 2/3was added. Then the flow-through was discarded and replaced the Filter Cartridge in the same Collection Tube. Spin the full assembly for 1 min to remove residual fluid. The Filter Cartridge was transferred into a fresh Collection Tube, A 100 µL aliquot of preheated (95°C) Elution Solution was placed at the center of the filter. Centrifugation was 20-30 seconds at maximum speed to RNA recovery (as in Figure 11). miRNA quantification was performed using a Nano Drop spectrophotometer which measured the concentration of RNA sample, indicating the A260 and A280 values, expressed in ng/µL

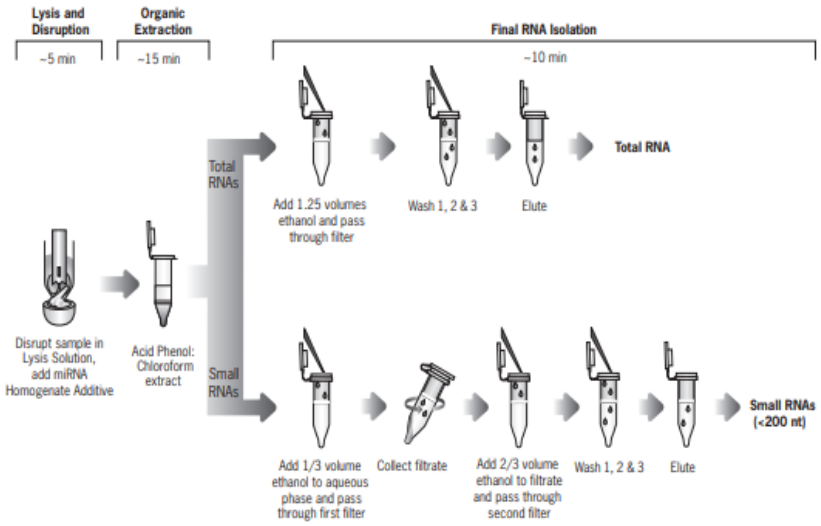

Figure 11- Overview of the mirVana™ miRNA Isolation Kit Procedure*. Initially, the sample gets lysed in a denaturing lysis solution that retains RNA integrity and inactivates the RNases. The lysate then undergoes a single extraction with Acid-Phenol: Chloroform. This extraction step eliminates most other cellular constituents, yielding a semi-pure RNA preparation. This preparation may then be further purified by means of a glass-fiber filter through either of the two methods, leading to the isolation of either total RNA or a size fraction enriched in miRNAs. The glass-fiber filter method uses buffering solutions meant to retain miRNAs, therefore greatly minimizing the loss of small RNAs due to conventional glass-fiber filter methods (Official Website: Thermo Fisher Scientific, n.d.).*

- ***Reserve transcription***

RNA Transcription was performed using the Thermo-Fisher datasheet (TaqMan TM Small RNA Assay): The reaction was prepared from 7 µL of the reaction mix (Table 6) and 5 µL of total RNA in a reaction tube. Each 5 µL sample contained 1-10 ng total RNA. The mixture was well mixed and briefly centrifuged to collect the contents at the bottom of the tubes. Next, 3 µL

of 5 X RT Primer was added to each reaction tube, followed quick spin The tubes were collected and placed on ice.

Component	Volume per reaction(1 reaction)
100 mM dNTPs(with dTTP)	0.15 µL
Multiscribe™ Reserve Transcriptase,50 U/µL	10 µL
10X Reserve Transcription Buffer	1.50 µL
RNase Inhibitor, 20 U/µL	0.19 µL
Nuclease-free water	4.26 µL
TOTAL REACTION MIX VOLUME	**7.00 µL**

Table 6- component of RT reaction Mix. *The RT reaction mix contains enzymes, dNTPs, and buffers necessary for the reverse transcription process. The RNA is the template that we are converting(Thermo Fisher Scientific, n.d.)*

Finally, the samples were set in a thermal cycler (Table 7) with a reaction volume of 15.0 µL. Thermo Scientific NanoDrop One/OneC Spectrophotometer quantified cDNA from RNA samples, measuring absorbance at 260 nm for nucleic acids concentration. The RT reaction was maintained at -20°C.

Step	Temperature	Time
Reverse transcription	16° C	3o minutes
	42° C	3o minutes
Stop reaction	85° C	5 minutes
Hold	4° C	Hold

Table 7- Thermo-Cycler Protocol for cDNA Synthesis: Steps, Temperatures, and Durations*. This table outlines the thermos-cycler protocol used for cDNA synthesis, including the temperatures and durations for each step: primer annealing, cDNA synthesis, enzyme inactivation, and preservation (Thermo Fisher Scientific, n.d.).*

- ***Real time PCR (RT-PCR)***

Real-time PCR was performed using the ViiA7 Real-Time PCR to amplify cDNA transcribed via a thermal cycler. U6 small nuclear RNA (RNU6-1) was used as a housekeeping gene to ensure reliable normalization in gene quantification. The PCR reaction mix was prepared in a total volume of 20 µL per well. Each well contained 1 µL of cDNA, combined with 19 µL of reaction mix :10 µL of No UNG Taq, 1 µL of TM, and 8 µL of nuclease-free water (Table 8).

Component	Volume reaction
TaqMan TM small RNA assay (20X)	1 µL
TaqMan TM universal Master Mix II,no UNG	10 µL
cDNA	1 µL
Nuclease- free water	8 µL

Table 8- PCR Reaction Mix Components and Volumes for cDNA Amplification in a 96-Well Standard Plate*(Thermo Fisher Scientific, n.d.)*

The instrument was configured with a block appropriate for the plate type used, which was a 96-well standard 0.1 mL plate (Table 8). The following thermal cycling protocol included UNG activation, Enzyme activation, Denaturation and Annealing for primer binding and DNA synthesis by 40 cycles (Table 9).

Step	Temperature	Time	Cycles
(optional) UNG activation	50° C	2 minutes	1
Enzyme activation	95° C	10 minutes	1
Denature	95° C	15 seconds	40
Anneal/Extend	60 ° C	60 seconds	

Table 9- Thermal Cycling Protocol for PCR Amplification: *Steps, Temperatures, and Durations. Thermal cycling protocol for PCR amplification, detailing the specific temperatures and durations for each step, including UNG activation, enzyme activation, denaturation, and annealing/extension(Thermo Fisher Scientific, n.d.)*

3.6 mRNA purification

- ***TRIzol™ reagent***

Splenocytes were resuspended in 1 mL of TRIzol and incubated for 5 minutes at room temperature. Chloroform (200 µL) was added to the sample, and vortexed for 30 seconds. Incubation for 5 minutes at RT to allow phase separation. The sample was centrifuged at 12000 g for 15 minutes at 4°C, and the upper aqueous phase (approximately 0.3-0.6 mL) was carefully transferred to a new sterile tube. RNA was precipitated by adding 0.25-0.3 mL isopropyl alcohol (5/6 of the aqueous phase volume) and mixing by gentle inversion. The sample was then incubated for 10 minutes at room temperature. Subsequently, it was centrifuged at 12000 g for 15 minutes at 4°C. RNA- pellet was washed once with 1 mL of 70% ethanol and centrifuged at 7500 g for 5 minutes at 4°C. RNA was air-dried for 30 minutes in a chemical hood, carefully avoiding over-drying. It was dissolved in 20-30 µL of nuclease-free water by gently pipetting up and down to facilitate dissolution without generating bubbles.

For mRNA concentration measurement, a Nano Drop spectrophotometer was used. The measured concentration (ng/µL) confirmed the amount of RNA in the analyzed sample, indicating its suitability and quality for future experiments.

- ***Reserve transcription***

The optimized protocol is designed to synthesize first-strand cDNA suitable for two-step Real-time PCR. The kit SuperScript™ VILO™ cDNA Synthesis Kit contained Reaction Mix, Enzyme Mix and DEPC-treated water, which was added based on the volume of RNA (see Table 10). For a single reaction, all components were mixed in a tube placed on ice. For multiple reactions, a master mix was prepared without RNA. The reaction mix was gently inverted and briefly centrifuged to ensure all contents were settled at the bottom of the tube.

Component	volume
5x-VILO TM reaction Mix	4 µl
10X superscript Enzyme Mix	2 µl
RNA(up to 2.5 µg)	X µl
DEPC-treated water	To 20 µl

Table 10- Reagents Provided with the Kit. *The essential components and volumes required for the preparation of the reaction mix used in mRNA isolation and downstream cDNA synthesis. It maintains clarity and scientific accuracy(Official Website: Thermo Fisher Scientific, n.d.).*

The reaction tubes were transferred into a thermal cycler, and temperature cycling was performed under standard parameters (Table 11). The Thermo Scientific NanoDrop One/OneC Spectrophotometer was used to quantify cDNA from RNA samples.

Step	Temperature	Time
Reverse transcription	25° C	10 minutes
	42° C	6o minutes
Stop reaction	85° C	5 minutes
Hold	4° C	Hold

Table 11- Thermo-Cycler Protocol for cDNA Synthesis: Steps, Temperatures, and Durations Overview.

- ***Real time PCR (RT-PCR)***

The cDNA, multiplied using a thermal cycler, was tasked with the ViiA7 Real-Time PCR System from Thermo Fisher Scientific. In RT-PCR, the quantification of genes involved comparing expression levels of target genes with those of housekeeping genes, remaining unchanged even under experimental treatment. In this study, Beta-Actin (BACT) (Mm02619580g1) was selected as the housekeeping gene(Juntang Lin & Christoph Redies, 2012) to normalize mRNA, Indeed, the analysis utilized probes targeting included IRAK1 (Mm01193538_m1), TRAF6 (Mm00493836_m1), FOXP(Mm00475162_m1), MYB (Mm00501741_m1), SMAD2 (Mm00487530_m1) and PTEN (Mm00477208_m1) to assess gene expression levels.

First, The PCR reaction mix (Table 12) was prepared and assembled in a final volume of 10 µL/well. 1 µL of cDNA was added to each well, followed by 5 µL of TaqMan® Universal Master Mix II (with or without UNG, 2X) and 1 µL of TaqMan® assay probes (20X) as indicated in Table 12. Each reaction also contained up to 100 ng of cDNA, adjusted to volume with RNase-free water.

Component	Volume reaction
TaqMan® universal Master Mix II , with / no UNG,2X	5 µL
TaqMan® Assay , 20 X	0.5 µL
Cdna or DNA template+ RNase-free water	1 µL
Nuclease- free water	3.5 µL

Table 12- Components and volumes of the PCR reaction mix utilized for cDNA amplification in a 96-well standard (0.1 mL) plate format*. The reaction mix comprises TaqMan Universal Master Mix (UNG), TaqMan assay probes, and nuclease-free water, combined with cDNA to achieve a total volume of 10 µL per well. The TaqMan probes were selected for their exceptional specificity and sensitivity in detecting the expression of target genes(Thermo Fisher Scientific, n.d.).*

This thermal cycling protocol categorizes Fast RT-PCR methods that were designed for rapid and efficient amplification while maintaining sensitivity and accuracy. The fast RT-PCR protocol included the following steps: initial denaturation at 95°C for 20-30 seconds, Denaturation at 95°C for 3-5 seconds per cycle, annealing at 60°C for 20-30 seconds per cycle, repeated for 40 cycles depending on experimental requirements (Referred to able 13).

Step	Temperature	Time
Initial Denaturation	95	0.5(20-30 Sec)
Denaturation(per Cycle)	95	0.1-0.2(3-5 Sec)
Annealing/Extension	60	0.3-0.5(20-30 Sec)
Total cycling Time(40 Cycles)	**-**	**~ 41 Min**

Table 13- Optimized Thermal Cycling Protocol for Fast PCR: Steps, Conditions, and Timing Parameters. *Thermal cycling protocol for PCR amplification, Temperature, and timing parameters for fast PCR, outlining each step's conditions and purpose in the amplification process. This protocol is optimized for rapid and efficient DNA amplification within approximately 41 minutes(Official Website: Thermo Fisher Scientific, n.d.).*

3.7 Statistical evaluation of experiment data

Experimental data were subjected to statistical analyses using Mann-Whitney, unpaired t test, one-way ANOVA, or Kruskal-Wallis tests, based on the normality distribution of data. Multiple comparison tests to assess intergroup differences were also performed. Statistical analyses and graphical representations of the data were performed with GraphPad Prism software (GraphPad Software, Inc, version 8.4.2).

4 Result

4.1 Efgartigimod treatment ameliorated EAMG clinical score

EAMG was induced in C57BL/6N mice by subcutaneous injections of TAChR. One week after the second boost, mice were treated twice weekly with intraperitoneal injections of either Efgartigimod or PBS (control group) for a total of 8 administrations (Figure 12, black arrows). Efgartigimod-treated mice showed milder symptoms compared with the PBS-EAMG mice starting from week 11 (after 5 administrations). At the end of experiment (week 13), Efgartigimod-treated mice had significantly lower disease score (mean 0.95± 0.17 SEM) compared to the control group (mean 1.83 ± 0.17 SEM; p=0.0024), suggesting that Efgartigimod dampened the EAMG symptoms (Figure 12).

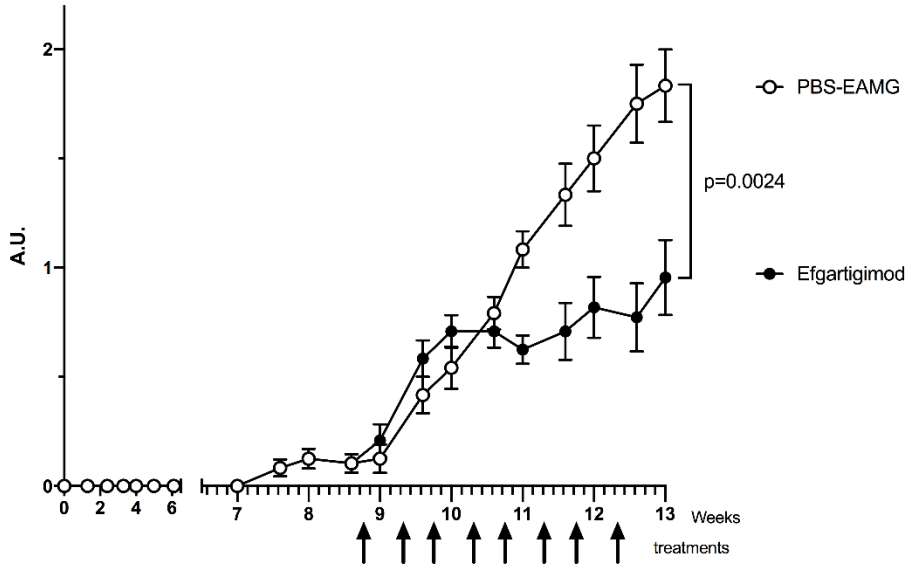

Figure 12- Effects of multiple administration of Efgartigimod on disease progression in EAMG. *Efgartigimod treatment alleviated disease severity in EAMG mice, showing reduction of symptom severity. Statistical analysis was performed using the Mann-Whitney test at week 13.*

Since EAMG is associated with increasing anti-AChR antibody levels, sera of mice collected at the end of the experiment were tested by RIA. The mean of 125I BTX-binding sites in PBS-EAMG group was 8.97 ± 0.69 SEM pmol/mL, while Efgartigimod-treated group showed lower titer (7.27 ± 1.07 SEM pmol/mL; p=0.0328) (Figure 13a). Moreover, the muscle AChR content resulted significantly higher in Efgatigimod treated-mice

(mean±SEM: 88.96± 37.52 fmol/g) compared to PBS-EAMG (mean±SEM: 12.79± 1.73 fmol/g) (Figure 13b).

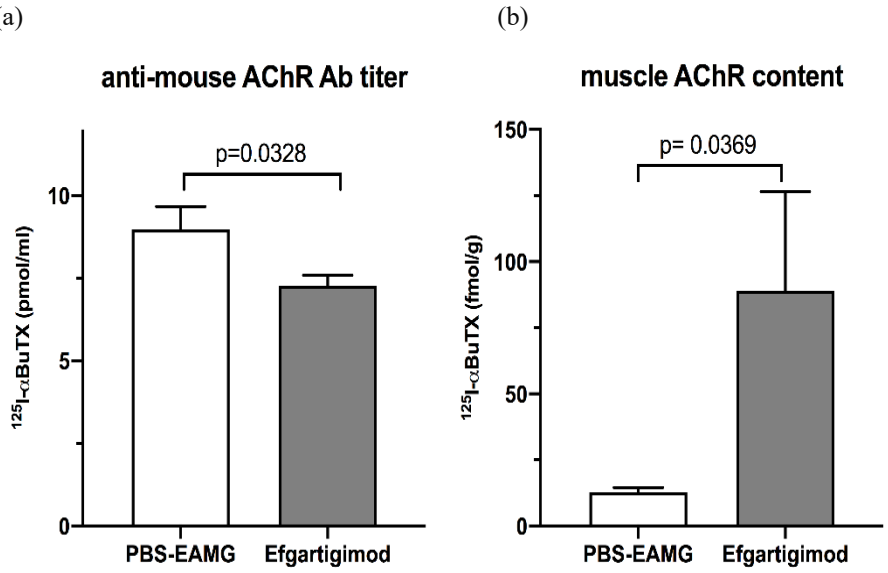

Figure 13- Impact of Efgartigimod on Anti-AChR antibody levels and musc AChR content. *Comparison of mean antibody concentrations and muscle ACl content (±SEM; n= 11) between Efgartigimod-treated and PBS-EAMG grou Statistical analysis was performed using unpaired t-test.*

These results suggested that Efgartigimod reduced circulating anti-mouse AChR antibody levels (beyond reducing IgG1 and IgG2b; data not shown) and, consequently, treated mice had higher content of AChR in muscles.

4.2 Efgartigimod modified splenic T and B cells populations.

It is noteworthy that Efgartigimod primary target is the FcRn, mainly expressed on endothelial cells of vessels. However, it is expressed also on cell membrane of immune cells (i.e. dendritic cells, macrophages, B cells). So, to evaluate the effects of Efgartigimod not only blocking the IgG recycling but also on immune cells populations, spleens of EAMG mice were harvested and immune cell phenotyping of splenocytes was performed by flow cytometry analysis.

Flow cytometric analysis of T cell populations was conducted in EAMG mice treated with Efgartigimod and both CD4+ T cells and CD8+ T cells subpopulations were analysed. Overall, there weren't statistical differences between groups in CD4+ T cells (p=0.07), CD4+CD44+CD62L- (p = 0.87), CD4+CD44+CD62L+ (p = 0.91) and CD4+CD44-CD62L+ T cells (p = 0.84). Flow cytometric analysis of CD8+ cells revealed a significant increase in CD8+T cell populations in Efgartigimod-treated group compared to PBS-EAMG mice (p= 0.0123). However, no statistically significant differences were found in subpopulations

CD8+CD44+CD62L- (p = 0.42), CD8+CD44-CD62L+ T cell (p = 0.85) or CD8+CD44+CD62L+ T cell (p = 0. 73). Overall, these data suggested that Efgartigimod did not have an impact on spleen T cells compartment (Figure 14).

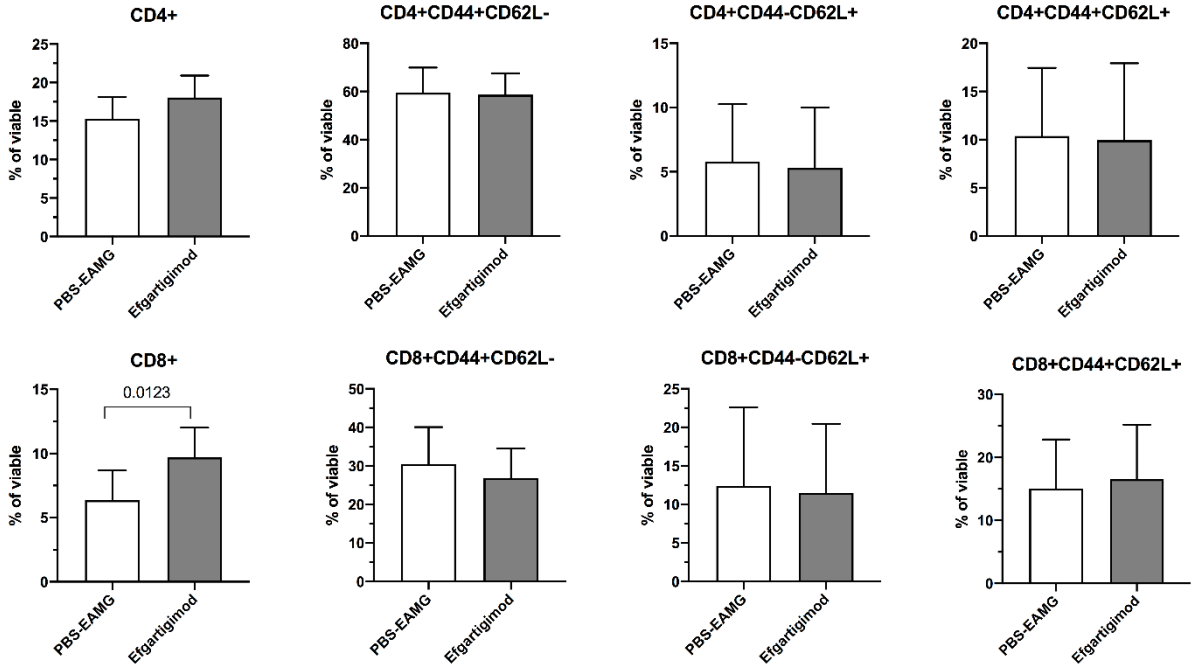

Figure 14- Flow cytometric analysis assessed the effect of Efgartigimod treatment on CD4⁺ and CD8⁺ T cell populations, *including effector memory ($CD44^+CD62L^-$), naïve ($CD44^-CD62L^+$) and central memory ($CD44^+CD62L^+$) subsets. Data (n=8) are represented as mean±SD and statistical analysis was performed using unpaired t test.*

B cells populations were also analysed by flow cytometry and data revealed significant changes in B cell compartment in Efgartigimod-treated mice. $CD19^+B220^+$ B cell population exhibited a statistically significant reduction compared to PBS-EAMG mice (p = 0.03). On the contrary, Efgartigimod treatment did not have a statistically significant effect on germinal center B cell populations ($CD19^+B220^+CD95^+GL7^+$). In contrast, PC $CD138^+TACI^+$ plasma cells displayed a substantial increase in Efgartigimod-treated mice, with statistical analysis confirming a significant difference between groups (p = 0.0002). In addition, also $P_{LL}CD138^+TACI^+CD19^-B220^-$ population showed a marked increase, with statistical analysis further supporting this solid rise (p = 0.0003) (Figure 15).

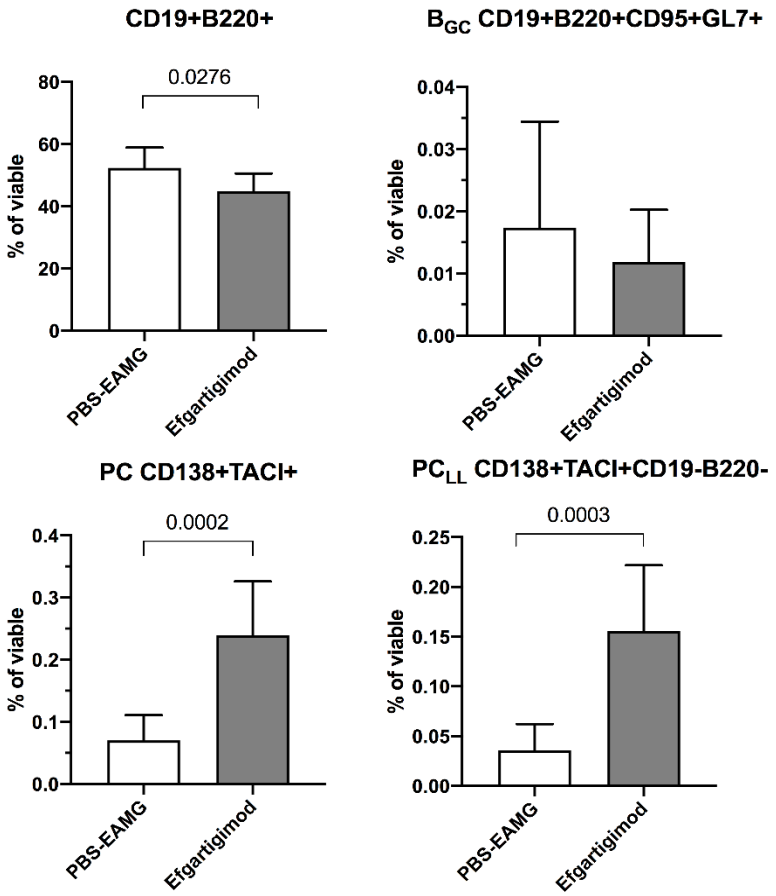

Figure 15- Flow cytometric analysis assessed the effect of Efgartigimod treatment on B cell populations, *including* $CD9^+B220^+$, $CD19^+B220^+CD95^+GL7^+$ *germinal center B cells,* $CD138^+TACI^+$ *plasma cells, and long-lived plasma cells* $CD138^+TACI^+CD19^-B220^-$. *Data (n=8) are represented as mean±SD and statistical analysis was performed using unpaired t test.*

4.3 Analysis of the expression profile of selected miRNA and their target in spleen

Since an immunomodulatory effect was observed in B cell compartment of spleen in Efgartigimod-treated mice, further preliminary analysis was conducted in a small number of mice to assess the impact of treatment on miRNAs levels, important molecules involved in lymphocytes maturation and activation. MiR-146a, miR-150 and miR-486 were selected for their involvement with the immune system functioning and modulation.

- ***miR-146a***

MiR-146a expression showed a mild increase both in EAMG and Efgartigimod groups, although not statistically significant compared to HD group (Figure 16a). Targets of miR-146a were analyzed to assess any variations in mRNA expression levels. The mRNA expression of IRAK showed an increase in Efgartigimod compared to HD and EAMG despite the lack of statistical significance (Figure 16b). TRAF6 mRNA was upregulated in EAMG group with

mean 0.28 ± 6.62 SEM, compared to the HD group. TRAF6 expression was also increased in the Efgartigimod group but not statistically significant compared to the other groups (Figure 16c).

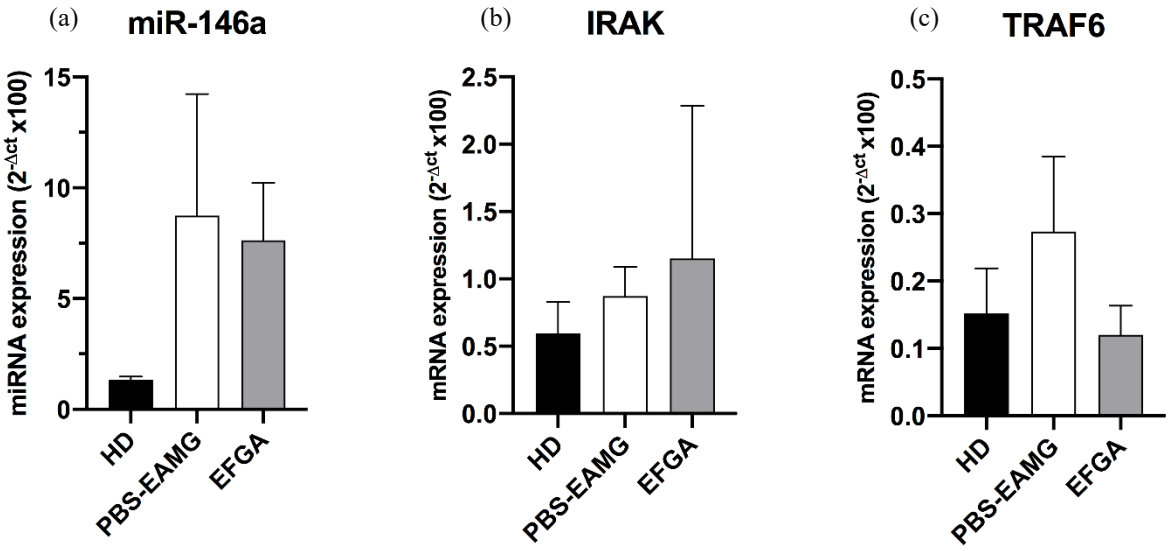

Figure 16- Expression levels of miRNA 146a and its target IRAK and TRAF6 in HD, EAMG mice and Efgartigimod-treated mice. *Data (at least 5 samples/group) mean ±SEM are represented, and statistical analysis was performed using Kruskal-Wallis test..*

- ***miR-486***

Another miRNA involved in immune cells regulation is miR-486. The expression of this miRNA was higher in the EAMG group compared to HD, but not statistically significant (Figure 17a). Treatment with Efgartigimod significantly reduced the expression level of this miRNA compared to untreated EAMG mice, suggesting that Efgartigimod was able to restore levels of miR486 in treated mice (Figure 17a).

Among target genes of miR486, SMAD2, a mediator of the TGF-beta signaling pathway and PTEN, a tumor suppressor gene that controls cell growth and maintains genomic stability, were selected. Both PBS-EAMG and Efgartigimod-treated mice did not present statistically significant differences compared with HD samples (Figure 17b and c).

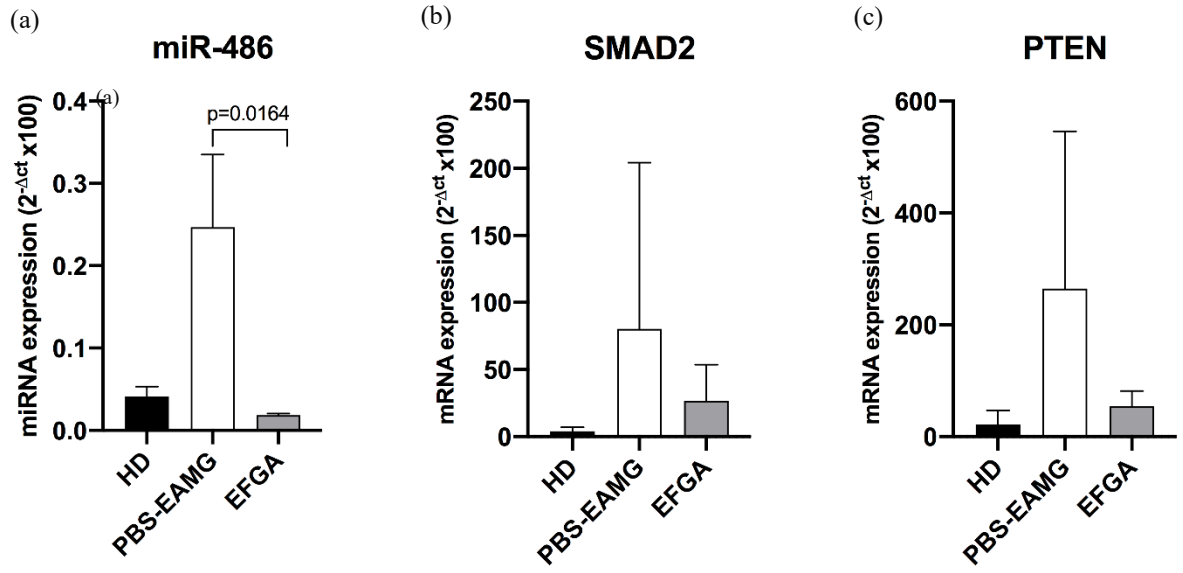

Figure 17- Expression levels of miRNA 486 and its target IRAK and TRAF6 in HD, EAMG mice and Efgartigimod-treated mice*. Data (at least 5 samples/group) mean±SEM are represented and statistical analysis was performed using Kruskal-Wallis test.*

- ***miR-150***

The expression of miRNA-150 showed a significant increase in the EAMG group compared to the HD group. Expression level in Efgartigimod-treated mice was lower than PBS-EAMG and no difference in expression of miR-150 was noted between the Efgartigimod-treated mice and the HD group, suggesting that treatment could downregulate this miRNA towards physiological levels (Figure 18a). Analysis of FOXP1 and MYB mRNA expression levels, did not revealed significant differences among groups (Figure 18b and c).

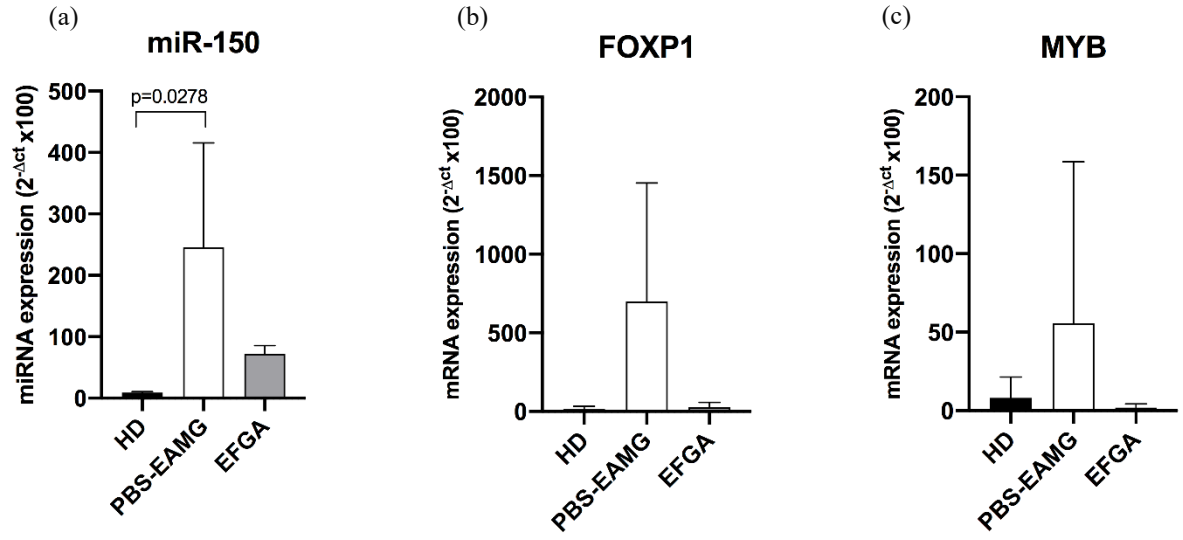

Figure 18- Expression levels of miRNA 150 and its target FOXP1 and MYB in HD, EAMG mice and Efgartigimod-treated mice*. Data (at least 5 samples/group) mean±SEM are represented, and statistical analysis was performed using Kruskal-Wallis test.*

5 Discussion

In recent years, an increasing number of new biological drugs have been developed for treatment of autoimmune diseases. Anti-FcRn drugs have been used as a valid and effective treatment, thanks to their unspecific mechanism of action which allow them to be applied in many autoimmune diseases, like MG. However, further studies could help to understand if these drugs could act on other molecular mechanisms. This project aimed at investigating the effects of the anti-FcRn Efgartigimod on the EAMG mouse model and in the modulation of the immune system. Indeed, just one study has been published about the effects of Efgartigimod in the animal model of Musk-MG, Efgartigimod improve muscle weakness in a mouse model for muscle-specific kinase myasthenia gravis(Huijbers et al., 2019), and its role in the immune system regulation has never been investigated, so far. In this project, it has been confirmed the efficacy of the anti-FcRn in significantly dampening the clinical symptoms of EAMG in treated mice (Figure 12) reducing circulating anti-AChR antibodies and protecting muscle AChR from degradation (Figure 13). This data sustains the efficacy of Efgartigimod in modulation of the EAMG, as already proven in MG patients and in the MuSK EAMG model (Huijbers et al., 2019).

Besides the known molecular mechanism of Efgartigimod, this research focused on the other immunomodulatory effects of this molecule. Indeed, FcRn is expressed also on the cell membrane of immune cells, and it has demonstrated its role in antigen presentation. Thus, Efgartigimod could inhibit this mechanism and reduce the activation of $CD4^+$ and $CD8^+$ T cells (Yihan Zhou & Shisong Jiang, 2023). Moreover, FcRn can influence the immune response by modulation of inflammatory cytokines (Shuo-Wang Qiao et al., 2008, Kristi Baker et al., 2014).

In our model, Efgartigimod induced a modest increase in $CD4^+$ and a significant increase in $CD8^+$ cells percentage in the spleen (Figure 14). No differences were observed in other T cells subpopulations, suggesting that Efgartigimod did not have an impact on these cells. On the contrary, results showed that Efgartigimod altered the B cells subset. Indeed, a significant reduction was observed on $CD19^+B220^+$ B cells percentage in the spleen (Figure 15). The observed decrease in the frequency of $CD19^+B220^+$ B cells could explain the increase in the frequency of $CD4^+$ and $CD8^+$ T cells as compared to PBS-EAMG, to maintain the total percentage of spleen cells. On the contrary, PC $CD138^+TACI^+$ and PC_{LL} $CD138^+TACI^+CD19^-B220^-$ population percentages were upregulated. Plasma cells were identified based on markers suggested in literature, useful to discriminate between PC and PC_{LL}(Katharina Pracht et al., 2017) . Indeed, while PC_{LL} are primarily located in the bone marrow, some studies have shown

that they can be found in the spleen in some autoimmune disease and the interaction between splenic PC_{LL} and follicular Thelper cells may contribute to the persistence of humoral autoimmunity(Eunkyeong Jang et al., 2016), Since the induction of these cells was not accompanied by an increase of anti-AChR level, it could be argued that these plasma cells may have a non-pathogenic phenotype. Indeed, a higher percentage of plasma cells could lead to an increment of autoantibodies in autoimmune diseases. However, it is now well recognized that plasma cells with a non-pathogenic phenotype, and specifically with immunoregulatory properties, may be generated under certain stimuli(Simon Fillatreau, 2018). This interesting result requires further analysis to elucidate this hypothesis *in vivo* and *in vitro*.

To further investigate the secondary effects of Efgartigimod in the immune system and B cell compartment, levels of miRNA involved in immune system modulation and in MG, were investigated in the spleen of mice. Mir146a is involved in regulating B-cell immune responses(Jennifer K. King et al., 2022). As reported in the serum of MG patients (Jiayin Lu et al., 2013), miR-146a was found to be upregulated also in the spleen of EAMG mice but not statistically significant and Efgartigimod treatment was not able to downregulate the level of miR-146a. Data in literature confirmed this trend in EAMG, showing the positive results obtaining silencing miR-146a (Y. , Zhang et al., 2014), No differences were observed in IRAK1 and TRAF6 mRNA expression levels.

MiR-150 plays a crucial role in the immune system modulation by targeting the main transcription factors involved in T and B lymphocyte maturation and differentiation (Natalie A. Bezman et al., 2011). In this study, it has been found a significant upregulation of miR-150 in spleen of PBS-EAMG mice compared to HD. In the context of EAMG, a higher level of miR-150 could promote T cell differentiation and sustaining the T cell immune response (Shengfang Xia et al., 2022). This increase is in line with the observations reported in literature that showed an increase level in serum of MG patients (Wenling Ao et al., 2020). Moreover, higher serum level of miR-150 was associated with an increase in circulating $CD19^+$ B cells, showing the multiple effects of miR-150(Yue-Zi Hu et al., 2023) Efgartigimod treatment downregulated the levels of miR-150 but the difference was not statistically significant, suggesting that the treatment, probably acting on B cell regulation, could influence also this miRNA slightly. Indeed, flow cytometry data demonstrated that mice treated with Efgartigimod had a lower percentage of $CD19^+$ $B220^+$ cells. However, no statistically significant differences were observed in the mRNA targets (MYB and FOXP1).

MiR-486 plays a key role in autoimmune diseases, especially MG, by modulating immune responses, inflammation, and muscle homeostasis. In the PBS-EAMG group, miR-486 was slightly upregulated compared to HD but not significantly, whereas Efgartigimod treatment significantly downregulated the levels, even lower than HD group. However, no differences were observed in its target (SMAD2, PTEN). In EAMG mice, dysregulation of miR-486 leads to modified immune homeostasis, promotes T-cell proliferation, macrophage activation, and increased cytokine secretion(Tetsuo Kiguchi et al., 2021). Studies have shown that miR-486 5p can suppress inflammatory responses in macrophages, suggesting its potential to dampen autoimmune process(Jianguo Hu et al., 2022). Since we observed a high variability in every group, more samples will be included in the analysis to strengthen the results obtained.

6 Conclusion

In this research, the effects of Efgartigimod were evaluated in the AChR EAMG mouse model for the first time, confirming its efficacy in dampen the clinical symptoms, thanks to a lower level of anti-AChR autoantibody concentration in serum and a higher content of muscle AChR of treated mice.

The impact of Efgartigimod was evaluated also on T and B cells subsets in spleen, revealing a decrease in $CD19^{+}B220^{+}$ B cells and a significant increase in PC subpopulations. Iinterestingly, these data suggest an effect of anti-FcRn also on B cells compartment that could be mediated by a direct binding of the drug to the FcRn expressed on B cells, or by an indirect effect linked to the reduction of circulating IgG. A time-point analysis of the variations in B cell percentage during the Efgartigimod administration and after a wash-out period could help to better understand its impact on B cells and specifically on PC. Moreover, further in vitro studies could clarify the mechanisms of action of Efgartigimod on B cells differentiation in PC.

The preliminary analysis of miRNA profile suggested a mild increase in miR-486 and miR-146a and showed a significant increase of miR-150 in EAMG mice. Treatment with Efgartigimod can restore levels of miR-150 but did not have a significant effect on the other miRNA analyzed. To better outline the secondary effects of an Anti-FcRn administration, additional studies should be conducted to corroborate this data and extend the analysis to more miRNA involved in the immune response.

Investigating other effects of Efgartigimod, beyond the inhibition of IgG recycling, can be useful to better understand the differences in interindividual treatment response.

7 References

Adrianna Douvris, Jose Viñas, & Kevin D. (2022). Burn, miRNA 486 5p: signaling targets and role in non malignant disease. Cellular and Molecular Life Sciences , 79(• https://doi.org/10.1007/s00018-022-04406-y.), 376.

Akira, S., Uematsu, S. ;, & Takeuchi, O. (2006). Pathogen recognition and innate immunity. Cell , 124, 783–801.

Alexander MS, Casar JC, Motohashi N, Myers JA, Eisenberg I, Gonzalez RT, Estrella EA, Kang PB, Kawahara G, & Kun kel LM. (2011). Regulation of DMD pathology by an ankyrin encoded miRNA. SK.

Alshekhlee A, Miles J.D, Katirji B, Preston D.C, & Kaminski H.J. (2009). Incidence and Mortality Rates of Myasthenia Gravis and Myasthenic Crisis in US Hospitals. Neurology, 72(doi: 10.1212/WNL.0b013e3181a41211.), 1548–1554.

Avidan N, Le Panse R, Berrih-Aknin S, & Berrih-Aknin S. (2014). Genetic basis of myasthenia gravis. A Comprehensive Review. J Autoimmun, 52, 146–153.

Balandina, S., Lecart, P., Dartevelle, A., Saoudi, S., & Berrih-Aknin. (2005). Functional defect of regulatory CD4(+)CD25+ T cells in the thymus of patients with autoimmune myasthenia gravis . Blood, 105, 735–741.

Bayés-Genis A, Lanfear DE, Ronde MWJD, Lupón J, Leenders JJ, Liu Z, Z. N., Eijkemans MJC, Zamora E, & Antonio MD. (2018). Prognostic value of circulating microRNAs on heart failure-related morbidity and mortality in two large diverse cohorts of general heart failure patients. . Eur J Heart Fail, 20(doi: 10.1002/ejhf.984), 67–75.

Beghi E, Antozzi C, & Batocchi AP. (1991). Prognosis of myasthenia gravis:a multicenter follow-up study of 844 patients. J Neurol Sci., 106, 213–220.

Benfaremo, D., Manfredi, L., Luchetti, M. M., & Gabrielli, A. (2018). Musculoskeletal and rheumatic diseases induced by immune checkpoint inhibitors: a review of the literature. Curr. Drug Safety , 13, 150–164.

Boldin, M. P., Taganov, K. D., Rao, D. S., Yang, L., Zhao, J. L., Kalwani, M., Garcia-Flores, Y., Luong, M., Devrekanli, A., & Xu, J. (2011). miR-146a is a significant brake on autoimmunity, myeloproliferation, and cancer in mice. J. Exp. Med, 208, 1189–1201.

Brito MB, Goulielmaki E, & Papakonstanti EA. (2015). Focus on PTEN regulation. Front Oncol , 5(https:// doi. org/ 10. 3389/ fonc.2015.00166.), 166.

Canan Ulusoy, F. Ç. (2017). Immunization with Recombinantly Expressed LRP4 Induces Experimental Autoimmune Myasthenia Gravis in C57BL/6 Mice.

Carmelo Rodolico, Carmen Bonanno, Antonio Toscano, & Giuseppe Vita. (2020). MuSK-Associated Myasthenia Gravis: Clinical Features and Management. Frontiers in Neurology, 11(660).

Carr AS, Cardwell CR, McCarron PO, & McConville J. (2010). A systematic review of population based epidemiological studies in myasthenia gravis. BMC Neurol, 18:10(doi: 10.1186/1471-2377-10-46), 46.

Chen D, Li H, Xie J, Zhan Z, Liang L, & Yang X. (2017). Herpes zoster in patients with systemic lupus erythematosus: clinical features, complications and risk factors. Exp Ther Med , 14, 6222–6228.

Chen, Y., Zeng, Z., Shen, X., Wu, Z., Dong, Y., & Cheng, J. C.-H. (2016). MicroRNA-146a-5p Negatively Regulates Pro-Inflammatory Cytokine Secretion and Cell Activation in

Lipopolysaccharide Stimulated Human Hepatic Stellate Cells through Inhibition of Toll-Like Receptor 4 Signaling Pathways. Int. J. Mol. Sci. , 17, 1076.

Chen, Y., Zhang, G., Chen, W., Qiu, Q., & Pan, Y. (2020). Plasma endothelial microvesicles and their carrying miRNA-155 serve as biomarkers for ischemic stroke. J. Neurosci. Res., , 98, 2290–2301.

Cunningham M, & Gilkeson G. (2011). Estrogen receptors in immunity and autoimmunity. Clin Rev Allergy Immunology, 40(doi: 10.1007/s12016-010-8203-5), 66–73.

Dana L.E. Vergoossen, Jaap J. Plomp, & Christoph Gstöttner. (2021). Functional monovalency amplifies the pathogenicity of anti-MuSK IgG4 in myasthenia gravis. Roceedings of the National Academy of Sciences (PNAS), 118(11).

Delves, P., & Roitt, I. (2000a). The immune system. Part 1. N Engl J Med, 3(49), 343.

Delves, P., & Roitt, I. (2000b). The immune system. Part 2. N Engl J Med, 343(3), 108–117.

D.M. Valenzuela, T.N. Stitt, P.S. DiStefano, E. Rojas, K. Mattsson, D.L. Compton, L. Nunez, J.S. Park, J.L. Stark, & D.R. Gies. (1995). Receptor tyrosine kinase specific for the skeletal muscle lineage: expression in embryonic muscle, at the neuromuscular junction, and after injury. Neuron, 15, 573–584.

ElKhouly AM, Youness RA, & Gad MZ. (2020). MicroRNA-486-5p and microRNA-486-3p: multifaceted pleiotropic mediators in oncological and non-oncological conditions. Non-coding RNA Res. MicroRNA-486-5p and microRNA-486-3p: multifaceted pleiotropic mediators in oncological and non-oncological conditions. Non-coding RNA Res. . J.Ncrna.2020.01.001. , 5, 11–21.

Eunkyeong Jang, Wang Sik Cho, Yeon-Kyung Oh, Mi-La Cho, Jung Mogg Kim, Doo-Jin Paik, & Jeehee Youn. (2016). Splenic Long-Lived Plasma Cells Promote the Development of Follicular Helper T Cells during Autoimmune Responses. The Journal of Immunology, 196(https://doi.org/10.4049/jimmunol.1401059), 1026–1035.

Fujii Y, Hashimoto J, Monden Y, Ito T, Nakahara K, & Kawashima Y. (1986). Specific activation of lymphocytes against acetylcholine receptor in the thymus in myasthenia gravis. J Immunol. .

Gasperi C, Melms A, & Schoser B. (2014). nti-agrin autoantibodies in myasthenia gravis. Neurology, 82, 1976–1983.

Gasperi, C., Melms, A., Schoser, B., Zhang, Y., Meltoranta, J., & Risson, V. (2014). Anti-agrin autoantibodies in myasthenia gravis. Neurology, 82(22), 1976–1983.

Gilhus NE, Verschuuren JJ, & Lancet Neurol. (2015). Myasthenia gravis: subgroup classification and therapeutic strategies. 14(doi: 10.1016/S1474-4422(15)00145-3), 1023–1036.

Gomez-Manzano C, Fueyo J, Jiang H, Glass TL, Lee H-Y, Hu M, Liu J-L, Jasti SL, Liu T-J, & Conrad CA. (2003). Mechanisms underlying PTEN regulation of vascular endothelial growth fac tor and angiogenesis. Ann Neurol , 53(https:// doi. org/ 10.1002/ana.10396), 109–117.

Grob D., Brunner N., Namba T., & Pagala M. (2008). Lifetime Course of Myasthenia Gravis. Muscle Nerve, 37(doi: 10.1002/mus.20950), 141–149.

Hakan Cetin, David Beeson, Angela Vincent, & Richard Webster. (2020). The Structure, Function, and Physiology of the Fetal and Adult Aetylcholine Receptor in Muscle. Sec. Molecular Signalling and Pathways, 13(https://doi.org/10.3389/fnmol.2020.).

Hamaguchi Y, Mori A, & Uemura T. (2015). Incidence and risk factors for herpes zoster in patients undergoing liver transplantation. Transpl Infect Dis , 17, 671–678.

Hans Frykman, & Pankaj Kumar. (2021). Laboratory Testing of Myasthenia Gravis: New Treatments Drive Change. Applied Labratory Medicine, 6(4), 1087–1089.

Hardy, R. R. (2004). B-1 B cell development. Journal of Immunology, 173(3), 1059–1064.

Hess GP. (1979). Acetylcholine-receptor-controlled ion fluxes in microsacs (membrane vesicles) obtained from the electroplax of Electrophorus electricus. In: Smith FO, Worden FG (Eds) The Neurosciences, Fourth Study Program. MIT Press, Cambridge, 831–839.

Higuchi O, Hamuro J, & Motomura M. (2011). Autoantibodies to low-density lipoprotein receptor-related protein 4 in myasthenia gravis. Ann Neurol, 69, 418–422.

Hobson-Webb LD, Benatar M, & Hehir MK. (2017). Rituximab as treatment for anti-musk myasthenia gravis: multicenter blinded prospective review. Neurology, 89, 1069–1077.

Hoch W., McConville J., Helms S, Newsom-Davis J., Melms A., & Vincent A. (22001). Auto-Antibodies to the Receptor Tyrosine Kinase MuSK in Patients with Myasthenia Gravis without Acetylcholine Receptor Antibodies. Nat. Med, 7(doi: 10.1038/85520), 365–368.

Howard, J. F., Bril, V., Vu, T., Karam, C., Peric, S., Margania, T., Murai, H., Bilinska, M., Shakarishvili, R., & Smilowski, M. (2021). safety, efficacy, and tolerability of efgartigimod in patients with generalised myasthenia gravis (ADAPT): A multicentre, randomised, placebo-controlled, phase 3 trial. The Lancet Neurology, 20, 526–536.

Hu Z, Chen JQ, Papp G, Póliska S, Szabó K, Tarr T, & Bálint BL. (2017). MicroRNA expression profiles identify disease-specific alterations in systemic lupus erythematosus and primary sjögren's syndrome. PloS One , 12(3)(doi: 10.1371/journal.pone.0174585).

Hubbard, S. R., & Gnanasambandan, K. (2013). Structure and activation of MuSK, a receptor tyrosine kinase central to neuromuscular junction formation. Biochim. Biophys. Acta , 1834, 2166–2169.

Huijbers, M. G., Plomp, J. J. , van Es, I. E., Fillié-Grijpma, Y. E., Kamar-Al Majidi, S., U. P., de Haard, H., Hofman, E., van der Maarel, S. M., & V., & J. J. G. M. (2019). Efgartigimod improves muscle weakness in a mouse model for muscle-specific kinase myasthenia gravis. Science Direct, 317, 133–143.

Huybrechts, Y., Boudin, E., Hendrickx, G., Steenackers, E., Hamdy, N., Mortier, G., Martínez Díaz-Guerra, G., Bracamonte, M. S., Appelman-Dijkstra, N. M., & Van Hul, W. (2022). Identification of Compound Heterozygous Variants in LRP4 Demonstrates That a Pathogenic Variant Outside the Third β-Propeller Domain Can Cause Sclerosteosis. Genes , 13, 80.

J. Zhang, Y. Chen, G. Jia, X. Chen, J. Lu, & H. Yang. (2013). FOXP3-3279 and IVS9+459 polymorphisms are associated with genetic susceptibility to myasthenia gravis . Neurosci Lett, 534, 274–278.

Janeway, C. A., Travers, P., Walport, M., & Shlomchik, M. J. (2001). Immunobiology: The Immune System in Health and Disease. Garland Science.

Jaretzki A, Barohn RJ, Ernstoff RM, Kaminski HJ, Keesey JC, & Penn AS. (2000). Myasthenia gravis: recommendations for clinical research standards. Task Force of the Medical Scientific Advisory Board of the Myasthenia Gravis Foundation of America. Neurology., 55, 16–23.

J.C. Keesey. (2002). Crisis in myasthenia gravis. An Historical Perspective. Muscle Nerve., 26, 1–3.

Jennifer K. King, Tiffany M. Tran, May H. Paing, Yuxin Yin, Amit K. Jaiswal, Ching-Hsuan Tso, Koushik Roy, David Casero, & Dinesh S. Rao2. (2022). Regulation of T-independent B-cell responses by microRNA-146a. Front. Immunol., 13(https://doi.org/10.3389/fimmu.2022.984302).

Jianguo Hu, Cheng Jin, Li Fang, Yao Lu, Yanying Wu, & Xiangfeg Xu. (2022). MicroRNA-486-5p suppresses inflammatory response by targeting FOXO1 in MSU-treated macrophages. Autoimmunity, 55(8), 661–669.

Jiayin Lu, Mei Yan, Yuzhong Wang, Junmei Zhang, Huan Yang, Fa-fa Tian, Wenbin Zhou, Ning Zhang, & Jing Li. (2013). Altered expression of miR-146a in myasthenia gravis. Science Direct, 55(https://doi.org/10.1016/j.neulet.2013.09.014), 85–90.

Juntang Lin, & Christoph Redies. (2012). Histological evidence: housekeeping genes beta-actin and GAPDH are of limited value for normalization of gene expression. Springer Nature Link, 222, 369–376.

Kaminski, H. J., Sikorski, P., Coronel, S. I., & Kusner, L. L. (2024). Myasthenia gravis. Journal of Clinical Investigation, 134(2).

Kao, J. C., Brickshawana, A., & Liewluck, T. (2018). Neuromuscular complications of programmed cell death-1 (PD-1) inhibitors. Curr. Neurol. Neurosci. Rep. , 18(63).

Kaori Noridomi, Go Watanabe, Melissa N. Hansen, Gye Won Han, & Lin Chen. (2017). Structural insights into the molecular mechanisms of myasthenia gravis and their therapeutic implications. ELife, 6(e23043, 2017. DOI: 10.7554/eLife.23043.).

Katharina Pracht, Julia Meinzinger, Patrick Daum, Sebastian R. Schulz, Dorothea Reimer, Manuela Hauke, Edith Roth, Drik Milenz, Claudia Berek, Joana corte real, & Wolfgang Schuh. (2017). A new staining protocol for detection of murine antibody-secreting plasma cell subsets by flow cytometry. European Journal of Immunology, 47(8), 1389–1392.

Koneczny I, Cossins J, & Vincent A. (2013). The role of muscle-specific tyrosine kinase (MuSK) and mystery of MuSK myasthenia gravis. J Anat., 224(doi: 10.1111/joa.12034), 29–33.

Kristi Baker, Timo Rath, Michal pyzik, & Richard S Blumberg. (2014). The Role of FcRn in Antigen Presentation. Frontiers in Immunology, 5(10.3389/fimmu.2014.00408), 408.

Lazaridis K, Vrolix K, Fraussen J, Losen M, Stevens J, & Molenaar PC. (2020). Clonal heterogeneity of thymic B cells from early-onset myasthenia gravis patients with antibodies against the acetylcholine receptor. J Autoimmun.

Leprince C, Cohen-Kaminsky S, Berrih-Aknin S, Vernet-Der Garabedian B, Hill ME, Shiono H, N.-D. J., & Willcox N. (1990). Thymic B cells from myasthenia gravis patients are activated B cells. Phenotypic and functional analysisThymic B cells from myasthenia gravis patients are activated B cells. Phenotypic and functional analysis. J Immunol.

Lutwyche JK, Keough RA, Hughes TP, & Gonda TJ. (2001). Mutation screening of the c-MYB negative regulatory domain in acute and chronic myeloid leukaemia. Br J Haematol, 114, 632–636.

Maartje G.M. Huijbers, Alexander F. Lipka, Jaap J. Plomp, Jaap J. Plomp, Silvère M. van der Maarel, & Jan J.G.M. Verschuuren. (2014). Pathogenic immune mechanisms at the

neuromuscular synapse: the role of specific antibody-binding epitopes in myasthenia gravis. Journal of Internal Medicine, 275(1), 12–26.

Mantegazza R, Meisel A, & Vu T. (2022). Terminal complement inhibitor ravulizumab in generalized myasthenia gravis. NEJM Evidence , 1–5.

Mantegazza Renato, Pia Bernasconi, & Paola Cavalcante. (2018). Myasthenia gravis: from autoantibodies to therapy. Curr Opin Neurol, 31(5)(doi: 10.1097/WCO.0000000000000596. PMID: 30156572,DOI: 10.1097/WCO.0000000000000596.), 517–525.

Marx.A, N. Willcox, M.I. Leite, W.Y. Chuang, B. Schalke, & W. Nix. (2010). Thymoma and paraneoplastic myasthenia gravis Autoimmunity. 43, 413–427.

McGuire LJ, Huang DP, Teoh R, Arnold M, Wong K, & Lee JC. (1988). Epstein–Barr virus genome in thymoma and thymic lymphoid hyperplasia. Patholo, 131, 385–390.

Mélanie A Cron, Solène Maillard, José Villegas, Frédérique Truffault, & Muriel Sudres. (2017). Thymus in volvement in early-onset myasthenia gravis. 13th International Conference on Myasthenia Gravis and Related Disorders. New York, United States, 10.111(nyas.13519. hal-01789833), 137–145.

Metchnikoff, E. (1887). Sur la lutta des cellules de l'organismes centre l'invasion des microbes. Annales Inst Pasteur Paris, 1, 321.

Michael H. Rivner, Brandy M. Quarles, & Jin Xiu Pan. (2020). Clinical features of LRP4/agrin-antibody–positive myasthenia gravis: A multicenter study. Muscle & Nerve, 62(3), 333–343.

Miriam L. Fichtner, Ruoyi Jiang, Aoibh Bourke, Richard J. Nowak, & Kevin C. (2020). Autoimmune Pathology in Myasthenia Gravis Disease Subtypes Is Governed by Divergent Mechanisms of Immunopathology. Frontiers in Immunology, 11(76).

Monticelli S, Ansel KM, & Xiao C. (2005). MicroRNA profiling of the murine hematopoietic system. Genome Biol, 6: R 71.

Monticelli S, Ansel KM, Xiao C, Socci NDSocci ND, Krichevsky AM, & Thai TH. (2005). MicroRNA profiling of the murine hematopoietic system. Genome Biol , 6(8)(R 71).

Morris O. Dailey. (2002). The Immune Functions of the Spleen. (P. 51–69. D. 10. 1007/978-1-59259-124-4_4. Chapter 4, Ed.).

Natalie A. Bezman, Tirtha Chakraborty, Timothy Bender, & Lewis L. Lanier. (2011). miR-150 regulates the development of NK and iNKT cells. JEM (Journal of Experimental Medicine), 208(https://doi.org/10.1084/jem.20111386), 2717–2731.

Newland AC, Sánchez-González B, Rejtő L, Egyed M, Romanyuk N, Godar M, Verschueren K, Gandini D, Ulrichts P, Beauchamp J, Dreier T, Ward ES, Michel M, Liebman HA, de Haard H, Leupin N, & Kuter DJ. (2019). Phase 2 study of efgartigimod, a novel FcRn antagonist, in adult patients with primary immune thrombocytopenia. American Journal of Hematology, 95, 178–187.

Official Website: Thermo Fisher Scientific. (n.d.). Thermo Fisher Scientific Inc. "Advancing Science for Life.

Oh IH, & Reddy EP. (1999). The myb gene family in cell growth, differentiation and apoptosis. Oncogene, 18, 3017–3033.

P. Strobel, W.Y. Chuang, S. Chuvpilo, A. Zettl, T. Katzenberger, & H. Kalbacher. (2008). Common cellular and diverse genetic basis of thymoma-associated myasthenia gravis.

Role of MHC Class II and AIRE Genes and Genetic Polymorphisms Ann N Y Acad Sci, 1132, 143–156.

Pasnoor, M., Dimachkie, M. M., Farmakidis, C., & Barohn, R. J. (2018). Diagnosis of Myasthenia Gravis. Neurol. Clin, 36, 261–274.

Payne AS, Ishii K, Kacir S, Lin C, Li H, & Hanakawa Y. (2005). Genetic and functional characterization of human pemphigus vulgaris monoclonal autoantibodies isolated by phage display. J Clin Invest. , 115(doi: 10.1172/JCI24185), 888–899.

Pevzner, B., Schoser, K., Peters, N. C., A. Karakatsani, B. Schalke, & Melms, S. (2012). Anti-LRP4 autoantibodies in AChR- and MuSK-antibody-negative myasthenia gravis. J. Neurol, 259, 427–435.

Phillips LH. (2004). The epidemiology of myasthenia gravis. . Semin Neurol., 24(1), 17–20.

Punga AR, Sabre L, Maddison P, Sadalage G, & Ambrose PA. (2018). Circulating microRNA miR-21-5p, miR-150-5p and miR-30e-5p correlate with clinical status in late onset myasthenia gravis. J Neuroimmunol, 321(doi: 10.1016/j.jneuroim.2018.05.003), 164–170.

Punga T, Bartoccioni E, Lewandowska M, Damato V, Evoli A, & Punga AR. (2016). Disease specific enrichment of circulating let-7 family microRNA in MuSK+ myasthenia gravis. J Neuroimmunol., 292(doi: 10.1016/j.jneuroim.2016.01.003), 21–26.

Punga T, Le Panse R, Andersson M, Truffault F, Berrih-Aknin S, & Punga AR. (2014). Circulating miRNAs in myasthenia gravis: miR-150-5p as a new potential biomarker. Ann Clin Transl Neurol, 1(doi: 10.1002/ acn3.24), 49–58.

Renato Mantegazza, & Fiammetta Vanoli. (2022). Efgartigimod: A First-in-class Investigational Antibody Fragment for the Treatment of Generalized Myasthenia Gravis. Neuromuscular Diseases.

Renato Mantegazza, James F, & Howard Jr. (2019). study of FcRn antagonist efgartigimod in generalized myasthenia gravis. MD, 92(23).

Robert L. Ruff, & Robert P. Lisak. (2018). Nature and Action of Antibodies in Myasthenia Gravis. Neurologic Clinics, 36(2), 275–291.

Romi F, Skeie GO, Gilhus NE, & Aarli JA. (2005). Striational antibodies in myasthenia gravis: reactivity and possible clinical significance. Archives of Neurology, 62(3), 442–446.

Rozen Le Panse, Sonia Berrih-Aknin, & et al. (2006). Thymic changes in early-onset myasthenia gravis: Role of cytokines and chemokines. Journal of Autoimmunity, 27(3), 217–229.

Santos, E., Coutinho, E., Moreira, I., Silva, A., Lopes, D., & Costa, H. (2016). Epidemiology of myasthenia gravis in northern Portugal: frequency estimates and clinical epidemiological distribution of cases. Muscle Nerve, 54(doi: 10.1002/mus.25068), 413–421.

Seybold M, & Lindstrom J. (1981). Patterns of acetylcholine receptorantibody fluctuation in myasthenia gravis. Ann NY Acad Sci, 377, 292–306.

Shengfang Xia, Jianqing Huang, Lijun Yan, Jiayi Han, Wenfeng Zhang, Hongwei Shao, Han Shen, Jinquan Wang, Changli Tao, Dingding Wang, & Fenglin Wu. (2022). miR-150 promotes progressive T cell differentiation via inhibiting FOXP1 and RC3H1. Science Direct, 83(11), 778–788.

Shuo-Wang Qiao, Kanna Kobayashi, Finn-Eirik Johansen, & Richard S. Blumberg. (2008). Dependence of antibody-mediated presentation of antigen on FcRn. PNAS, 105(https://doi.org/10.1073/pnas.0801717105), 9337–9342.

Simon Fillatreau. (2018). Natural regulatory plasma cells. Science Direct, 55, 62–66.

Small EM, O'Rourke JR, Moresi V, Sutherland LB, McAnally J, Gerard RD, Richardson JA, & Olson EN. (2010). Regulation of PI3-kinase/Akt signaling by muscle-enriched microRNA-486. PNAS, 107(doi: 10.1073/pnas.1000300107doi: 10.1073/pnas.1000300107), 4218–4223.

Tetsuo Kiguchi, Yoshito Kakihara, Manabu Yamazaki, Kouji Katsura, Kenji Izumi, Jun-ichi Tanuma, & Jun-ichi Tanuma. (2021). Identification and characterization of R2TP in the development of oral squamous cell carcinoma. Science Direct, 548, 161–166.

Treuting, P. M. (2018). Comparative Anatomy and Histology:A Mouse and Human Atlas. . Elsevier.

T.Rossen, & Rousseff. (2021). Diagnosis of Myasthenia Gravis. MDPI Journal, 10(8), 1736.

Uzawa A, S Kuwabara, S Suzuki, T Imai, H Murai, Y Ozawa, M Yasuda, Y Nagane, & K Utsugisawa. (2021). Roles of cytokines and T cells in the pathogenesis of myasthenia gravis. Clinical and Experimental Immunology, 203(3), 366–374.

von Andrian UH, & Mempel TR. (2003). Homing and cellular traffic in lymph nodes. Nat Rev Immunol , 3, 867–878.

Wang Z-Y, Qiao J, Melms A, & Link H. (1993). T cell reactivity to ace-tylcholine receptor in rats orally tolerized against experi-mental autoimmune myasthenia gravis. (pp. 394–404).

Wenling Ao, Canhui Tian, Xiongjun He, Yeli Hu, Weidong Wang, & Yajie Liu. (2020). Upregulation of miR150-5p in generalized myasthenia gravis patients is associated with decreased serum levels of IL-17 and increased serum levels of IL-10. Biomed Pap Med Fac Univ Palacky Olomouc Czech Repub., 164(1 DOI: 10.5507/bp.2019.009), 57–62.*

WHO. (2015). WHO Classification of Tumours of the Lung, Pleura, Thymus and Heart. 4th Ed. Lyon, IARC.

Witzemann V, Geuder K, Marx A, Schalke B, Toyka K, Kirch-ner T, & Muller-Hermelink H. (1992). Pathogenic significance of fetal-type acetylcholine receptors on thymic myoid cells in myas-thenia gravis. Dev Immunol , 2, 69–75.

Xiao C, Calado DP, Galler G, Thai T-H, Patterson HC, & Wang J. (2007). MiR 150 Controls B cell differentiation by targeting the transcription factor c-Myb. Cell. 131(doi: 10.1016/j.cell.2007.07.021), 146–159.

Xiaohua Yan, Ziying Liu, & Yeguang Chen. (2009). Article Navigation Journal Article Regulation of TGF-β signaling by Smad7. Oxford Academic, 41(4), 263–272.

Yan F, Chen Z, Wang H, Xia Y, & Lu Y. (2018). Therapeutic potential of mesenchymal cell-derived miRNA-150-5p-expressing exosomes in rheumatoid arthritis mediated by the modulation of MMP14 and VEGF. J Immunol , 201 (8)(doi: 10.4049/jimmunol.1800304), 2472–2482.

Yihan Zhou, & Shisong Jiang. (2023). Roles of FcRn in Antigen-Presenting Cells during Autoimmunity and a Clinical Evaluation of Efgartigimod as an FcRn Blocker. MDPI, 817(https://doi.org/10.3390/pathogens12060817).

Yue-Zi Hu, Qiao Li, P.-F. W., Xue-Ping L, & Zhao-Lan Hu. (2023). Multiple functions and regulatory network of miR-150 in B lymphocyte-related diseases. Front. Oncol, Sec. Molecular and Cellular Oncology, 13(https://doi.org/10.3389/fonc.2023.1140813).

Z.B. Hu, Y. Zhang, K.L. Ma, Y.X. Gong, G.H. Wang, L. Liu, J. Lu, P.P. Chen, C.C. Lu, X.Z. Ruan, & B.C. Liu. (2018). Platelet microparticles mediate glomerular endothelial injury in early diabetic nephropathy. J. Am. Soc. Nephrol, 29, 2671–2695.

Zhang, S., Q. Wang, T. Suzuki, & W.C. Xiong. (2008). LRP4 serves as a coreceptor of agrin. Mei Neuron, 60, 285–297.

Zhang, Y. , Li, x., Xu, Q., Gui, C. , & Wang, J. ,. (2014). Silencing miR-146a influences B cells and ameliorates experimental autoimmune myasthenia gravis. Journal of Neuroimmunology, 271, 50–57.

Zhao C, Pu M, & Chen D. (2021). Effectiveness and safety of Rituximab for refractory myasthenia gravis: a systematic review and single-arm meta-analysis. . Front Neurol, 736190, 12.

Zhong H, Zhao C, & Luo S. (2019). HLA in myasthenia gravis: From superficial correlation to underlying mechanism. . Autoimmun Rev, 18(9).

Zhou B, Wang S, Mayr C, Bartel DP, & Lodish HF. (2007a). miR 150, a microRNA expressed in mature B and T cells, blocks early B cell development when expressed prematurely. Proc Natl Acad Sci USA, 104, 7080–7085.

Zhou B, Wang S, Mayr C, Bartel DP, & Lodish HF. (2007b). miR-150, a microRNA expressed in mature b and T cells, blocks early b cell development when expressed prematurely. . Proc Natl Acad Sci United States America , 104(17), 7080–7085.

Zhou H, Hasni SA, Perez P, Tandon M, Jang SI, & Zheng C. (2013). miR-150 promotes renal fibrosis in lupus nephritis by downregulating SOCS1. J Am Soc Nephrol , 24(7)(doi: 10.1681/ASN.2012080849.), 1073–1087.

Zisimopoulou P, Brenner T, & Trakas N. (2013). Serological diagnostics in myasthenia gravis based on novel assays and recently identified antigens. Autoimmun Rev, 12, 924–930.

Zisimopoulou P, Evangelakou P, & Tzartos J. (2014). A comprehensive analysis of the epidemiology and clinical characteristics of anti-LRP4 in myasthenia gravis. J Autoimmun, 52, 139–145.